Bulletin of Volcanology (2026) 88:66
https://doi.org/10.1007/s00445-026-01987-5

RESEARCH

Growth and erosion of volcanic islands since 1963 analyzed by multi-sensor satellite data and historical records

Simon Plank[1] · Ronni Grapenthin[2] · Hannah R. Dietterich[3] · Ulrich Kueppers[4] · Francesco Marchese[5] · Nicola Pergola[5] · Emanuele Ciancia[5] · Nicola Genzano[6] · Franz J. Meyer[2] · Sandro Martinis[1] · Hannes Taubenböck[1,7] · Tobias Ullmann[7] · Thomas R. Walter[8]

Received: 20 December 2025 / Accepted: 8 May 2026 / Published online: 25 May 2026

Abstract
Most volcanic activity is taking place in the oceans. Depending on water depth, eruption recurrence times and volumes, a new island can form. The power of erosional forces, the type of erupted material and the efficiency of secondary processes determine the island's lifetime. Since the famous eruption of Surtsey (Iceland) in 1963, at least another 23 volcanic islands have appeared. Some islands remained intact for years or decades, whereas others disappeared within just weeks or months. In this study, we analyzed satellite data to determine growth and erosion rates of the volcanic edifices related to these 24 islands. We combined multi-sensor (optical, thermal, radar) satellite data time series with information from literature and the Global Volcanism Program database. We developed a comprehensive dataset, including 19 parameters, on the islands' lifetime, shape, area, volume, eruption style and duration, environmental conditions, development of sedimentary deposits, and the geomorphic evolution of the island over time. Our dataset is available in a database format. This database allows us to test eight hypotheses about factors influencing the islands' lifetime. Our results show that instead of one single critical factor, a combination of different factors influences the life history of volcanic islands. For instance, we show that larger islands do not necessarily live longer. The mechanical properties of the eruption products affect the island's structural integrity. Irrespective of the material, a minimum initial area of around 50,000 m^2 seems to be a reasonable threshold to give the island a chance to exist longer.

Keywords Volcanic islands · Multi-sensor remote sensing · Submarine eruptions · Surtseyan · Lifetime · Erosion

Introduction

Construction and erosion of volcanic islands is part of a natural cycle. There exist countless remnants of volcanic islands worldwide. It is striking that there is a considerable difference in the lifetime of the volcanic islands that formed

Editorial responsibility: A. Tibaldi

✉ Simon Plank
simon.plank@dlr.de

1 German Remote Sensing Data Center, German Aerospace Center DLR, 82234 Oberpfaffenhofen, Germany

2 Geophysical Institute and Department of Geosciences, University of Alaska Fairbanks, Fairbanks, AK 99775, USA

3 U.S. Geological Survey, Alaska Volcano Observatory, Anchorage, AK 99508, USA

4 Department of Earth and Environmental Sciences, Ludwig-Maximilians-Universität (LMU) Munich, 80333 Munich, Germany

5 Institute of Methodologies for Environmental Analysis, National Research Council, Tito Scalo, 85050 Potenza, Italy

6 Department ABC (Architecture, Built Environment and Construction Engineering), Politecnico Di Milano, Via Ponzio 31, 20133 Milan, Italy

7 Earth Observation Research Cluster, University of Würzburg, 97074 Würzburg, Germany

8 GFZ Helmholtz Centre for Geosciences, 14473 Telegrafenberg, Potsdam, Germany

in the past centuries. While some islands remain above sea level, others have eroded within weeks to years and disappeared below sea level. Here, we define the island's lifetime as the time from its first appearance above sea level to the time the island is no longer recognizable above sea level.

Explosive volcanic eruptions typically form islands of loose, unconsolidated tephra, which provide little resistance to wave erosion, leading to quick disappearance of the islands. A well-known example of a short-lived island, consisted of unconsolidated tephra, is Graham Island (also called Isola Ferdinandea), formed in 1831 offshore of Sicily (Cavallaro and Coltelli 2019).

However, several processes may add to the mechanical strength of a newborn island: (1) coverage by lava flows, (2) (partial) welding due to lava flows or shallow intrusions (Schmidt and Schmincke 2002), and (3) secondary mineral growth, as glassy volcanic ash (especially ash of basaltic composition) is very reactive to water (palagonitization).

The still existing Surtsey Island, formed off the south coast of Iceland during a 3.5-year long eruption, that began on November 14, 1963, is a good site to study these processes (Óskarsson et al. 2020). Surtsey became the type location for "Surtseyan" eruptions (Walker 1973)—a process that commonly forms volcanic islands. These eruptions are characterized by explosive activity (phreatomagmatic/hydrovolcanic) when ascending magma is coming into intimate contact with external water under confinement. The associated quenching of magma and steam formation typically forms angular and glassy clasts (Zimanowski et al. 2015). Five months later, the eruption style changed to predominantly effusive. Lava flows draped the pyroclastic material and strongly reduced the erosion rate (Thorarinsson 1964; Fridriksson 1975; Decker and Decker 1981). In addition, hydrothermal activity and low-temperature (< 100 °C) alteration of the previously unconsolidated basaltic glass (Prause et al. 2022) into consolidated palagonite tuff increased the resistance to wave erosion (Jackson et al. 2024).

Island evolution consists of several stages from seamount to island building, followed by island erosion (Schmidt and Schmincke 2000). Critical factors in the formation of a new volcanic island in shallow-water are: *the bulk volume of material erupted*, *the eruption rate*, *the eruption duration*, *fluctuations in eruption rate*, and *the effectiveness of erosion processes* (e.g., Nunn 1994). Volcano-tectonic structures may destabilize (location on active fault) or stabilize (solidified intrusions) an emerging island (Schmidt and Schmincke 2000). Factors influencing erosion processes on volcanic islands include the geologic setting, the local bathymetry, the climate, and especially the material of which the island is formed (Nunn 1994; Ramalho et al. 2013; Perron 2017). Documenting these parameters and processes can help describe the lifecycle of emergent volcanic islands.

In this study, we integrate multi-sensor (thermal, optical, Synthetic Aperture Radar (SAR)) satellite data time series (available since the 1980s, Fig. 2a) with information derived from reports on single volcanic events (available in the literature and the Global Volcanism Program (2025a) database). Using a statistical approach, we investigated volcanic islands with a range of eruptive styles and settings formed since 1963.

Investigated newly formed volcanic islands

Worldwide, at least 23 volcanic islands formed since the "birth" of Surtsey in 1963 (Fig. 1). Some of them were very short-lived on a human time-scale, i.e., they existed a few weeks or months only, while others resisted against ocean erosion for several years or even decades (Fig. 2b).

Against this background, the question arises: What influence do the various factors have that determine how long a newly formed volcanic island exists?

We investigated 24 volcanic islands at 12 volcano systems worldwide (Fig. 1, Table 1): *Surtsey*, *Sholan*, *Jadid*, *Home Reef*, *Late'iki*, *Hunga*, *Kuwae*, *Kavachi*, *Fukutoku-Oka-no-Ba*, *Iwo Jima*, *Nishinoshima* and *Bogoslof*. We developed a database including 19 parameters for these 24 islands (cf. "Data and methods" section, Table 2, Supp-Tab. 1). Some islands were formed during eruptions that lasted over 1 year or even several years. We named the islands after the start year of the eruption that formed the island, i.e., "Bogoslof 2016" (cf. Fig. 2b).

Satellite observations for monitoring newly formed volcanic islands

Earth observing satellites allow for global monitoring, which enables observations of volcanoes located in remote areas (Poland et al. 2020). Detecting and monitoring the evolution of a newly formed volcanic island requires satellite sensors with a spatial resolution appropriate to the island's size and area. Figure 2a provides an overview about the timeline of satellite missions and their spatial resolution since the launch of the first Landsat satellite in 1972. However, the early Landsat satellites did not provide systematic global coverage. Remote areas, where most of the newly formed volcanic islands are located, were not or very rarely imaged. Thus, short-lived islands formed in the 1970s are likely absent from the satellite record. Although coverage, observation frequency, and spatial resolution increased with the launch of Landsat 4/5 in 1982/1984, some short-lived islands that formed in the 1980s–2000s were not captured by satellites at all, while for other islands, satellite images with a suitable spatial resolution were acquired only several years after the islands' formation (Fig. 2a).

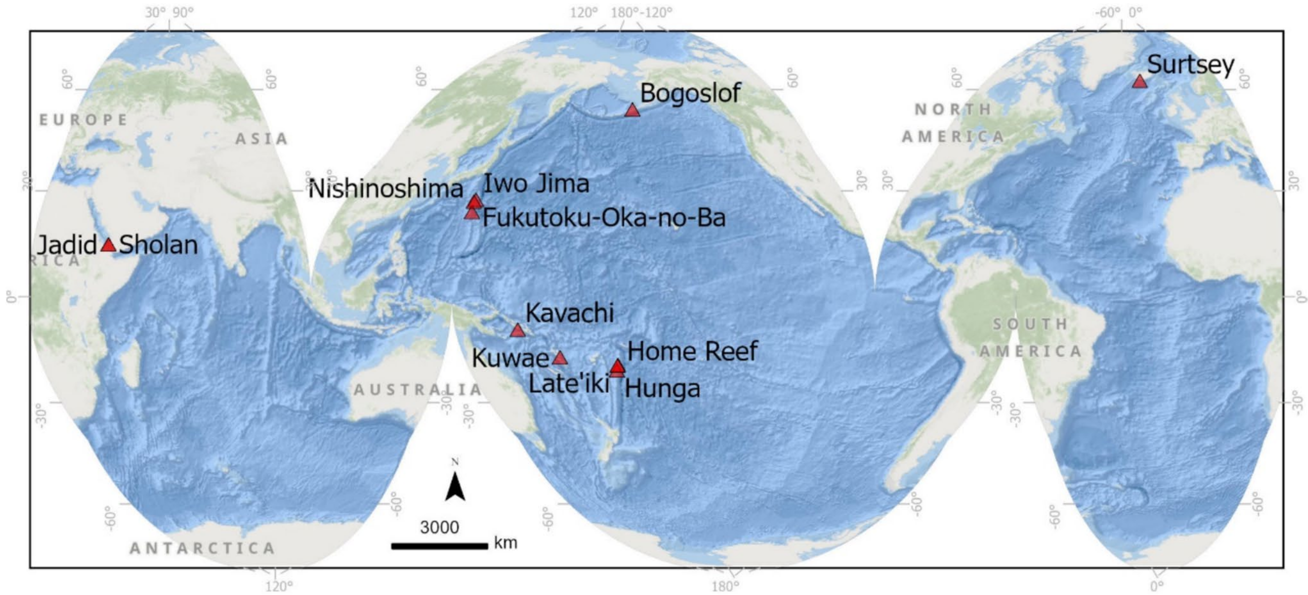

Fig. 1 Investigated volcanic islands. Background ESRI Basemap

More recent satellite capabilities make the detection of newly formed islands easier because of increased spatial and temporal resolution. Constellations of satellites with high spatial resolution such as PlanetScope, a constellation of ca. 130 cubesats (3 m), enables daily imaging of the majority of the Earth's landmass (PlanetLabs 2025)). But, the observation frequency in remote areas, where many island-forming volcanoes are located, is much lower.

Modern very high spatial resolution (VHR, < 1 m) commercial optical sensors, such as Pléiades or WorldView and successors, have capabilities for generating digital surface models (DSMs) from stereo images. This permits detailed 3-dimensional investigation and volume measurements of newly formed islands (Garvin et al. 2018). These satellites require manual data tasking. This, and the high costs of operational monitoring large areas for short-lived remote phenomena like new volcanic island formations, requires the combination of data from VHR sensors with the systematically acquired Landsat and Sentinel-2 data (10–15 m).

Especially in maritime regions with very high cloud cover probability, or at high latitudes with limited daylight during winter, the combination of optical with the weather and daylight independent VHR SAR sensors enables a high observation frequency (several days) for the detection and analysis of the evolution of newly formed volcanic domes (Walter 2023), crater morphology changes (Angarita et al. 2022), or volcanic islands (Plank et al. 2025), even in remote areas. SAR interferometry (InSAR) enables the generation of DSMs and thus the volume estimation of lava flows (Poland 2014; Plank et al. 2023) or islands (Xu et al. 2015).

Infrared sensors such as MODIS (Moderate Resolution Imaging Spectroradiometer) and VIIRS (Visible Infrared Imaging Radiometer Suite) enable the systematic detection of volcanic thermal anomalies on a global scale (Wright 2016; Coppola et al. 2019). Their high observation frequencies with 12 overpasses per day at the equator enable the monitoring of short-term changes of thermal activity at newly formed volcanic islands (Plank et al. 2020, 2025). Near real-time monitoring with infrared sensors on geostationary satellites such as Himawari, Meteosat, or GOES (Geostationary Operational Environmental Satellite) can provide precise timing of the onset of an eruption (Genzano et al. 2023). However, the geostationary sensors are mainly suited for the analysis of larger volcanic activity in mid to low latitudes.

The hypotheses

Island formation and persistence are influenced by a range of geological and environmental processes. Accordingly, we formulate and test the following hypotheses:

H1: The larger the initial island, the longer is the lifetime of an island (Nunn 1994).
H2: Due to shorter coastline length, compact circular islands withstand erosion better than irregular islands.
H3: Islands formed during long-lasting eruptions have a longer lifetime.
H4: Islands that grew during several eruptive episodes have a longer lifetime.

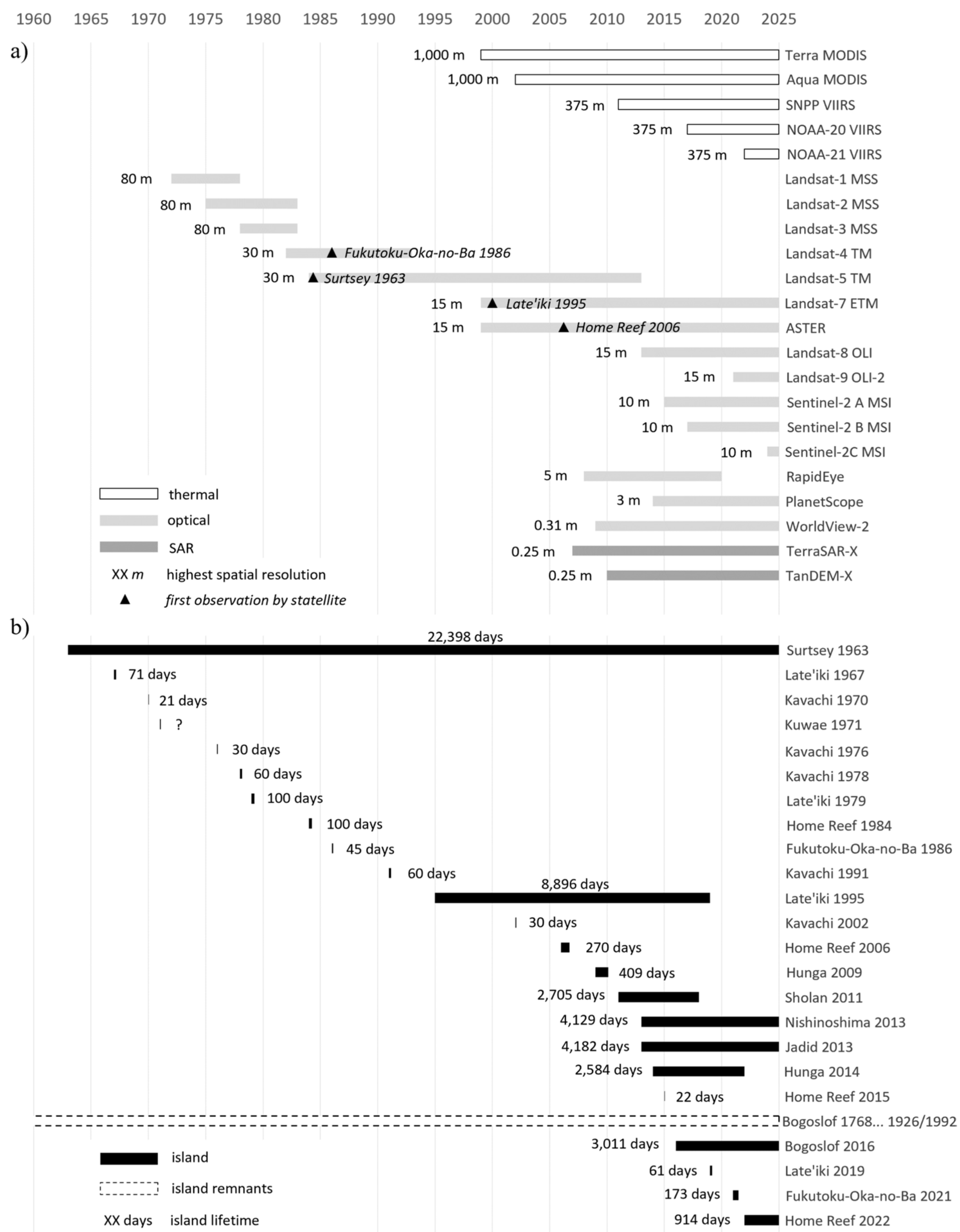

Fig. 2 **a** Timeline of available satellite sensors and their highest spatial resolution: MODIS (Moderate Resolution Imaging Spectroradiometer), VIIRS (Visible Infrared Imaging Radiometer Suite), MSS (Multispectral Scanner), TM (Thematic Mapper), ASTER (Advanced Spaceborne Thermal Emission and Reflection Radiometer), MSI (Multispectral Imager), OLI (Operational Land Imager). **b** Timeline of island lifetime

H5: The eruption style and products determine the island's lifetime (e.g., Nunn 1994).

H6: Hydrothermal alteration of unconsolidated pyroclastic material to palagonite tuff increases islands' resistance to wave erosion (e.g., Jakobsson et al. 2000; Heap et al. 2025).

H7: Islands protected by already existing neighboring islands or by accumulated sediments have a longer lifetime.

H8: The environmental conditions, height of sea waves and wind, etc. influence the islands' lifetime.

Data and methods

To analyze the evolution of newly formed islands ("Investigated newly formed volcanic islands" section), we investigated the satellite data shown in Fig. 2a, together with the information available in the scientific literature and in reports of the Global Volcanism Program (2025a). The following 19 main parameters were derived for each island (Tables 1 and 2).

Table 1 Investigated volcanic islands, their tectonic and geological setting (based on GVP = Global Volcanism Program 2025a) as well as information sources for area, height and volume

Tectonic setting	Tectonic region	Volcano and *abbreviation* (LAT/LON)	Year(s) of island formation (* still existing)	Rocks	Volcano type	Information source of				
						General	Maximum initial island area	Evolution of island area	Height	Volume
Rift zone	Iceland Neovolcanic Rift	Surtsey (63.30°N, 20.60°W)	1963*	Alkaline olivine basalt/ Picro-Basalt	Fissure vent(s), Pyroclastic cone(s), Tuff cone(s)	Kokelaar 1983; Global Volcanism Program 2025a	Óskarsson et al. (2020)	Landsat 5/7/8/9, Sentinel-2, Planet, TerraSAR-X	Óskarsson et al. 2020	
	Red Sea Rift	Jadid (15.09°N, 42.13°E)	2013*	Basalt/Picro-Basalt, Trachybasalt/Tephrite Basanite	Fissure vent(s), Pyroclastic cone(s), Shield	Xu et al. 2015, Global Volcanism Program 2025b	WorldView, Landsat 8, Xu et al. 2015	Landsat 8, TerraSAR-X, Planet	TanDEM-X, Xu et al. 2015	
		Sholan (15.16°N, 42.09°E)	2011							
Subduction zone	Tofua Volcanic Arc	Home Reef (*HR*) (18.99°S, 174.77°W)	1984	Dacite	Stratovolcano	Mantas et al. 2011; Plank et al. 2025; Global Volcanism Program 2025c	Global Volcanism Program 2025c			Estimated based on rectangular shape: 2 peaks with a crater in between
			2006				Global Volcanism Program (Global 2025c)	ASTER, Landsat 7	Global Volcanism Program 2025c	Estimated based on cone
			2015				RapidEye		Not available	No estimate possible
			2022*				TerraSAR-X, Plank et al. 2025	TerraSAR-X, Sentinel-2, Landsat 8/9	Plank et al. 2025	
		Late'iki (19.18°S, 174.87°W)	1967	Dacite	Stratovolcano	Melson et al. 1970; Plank et al. 2020; Yeo et al. 2022; Global Volcanism Program (Global 2025d)	Global Volcanism Program (Global 2025d)			Estimated based on mean of half ellipsoid and cuboid
			1979							
			1995				Global Volcanism Program 2025d	Landsat 7/8, Sentinel-2	Global Volcanism Program 2025d	
			2019				Sentinel-2, Plank et al. 2020	Sentinel-2, Landsat 8, TerraSAR-X	Not available	No estimate possible

Table 1 (continued)

Tectonic setting	Tectonic region	Volcano and *abbreviation* (LAT/LON)	Year(s) of island formation (* still existing)	Rocks	Volcano type	Information source of				
						General	Maximum initial island area	Evolution of island area	Height	Volume
		Hunga (20.55°S, 175.38°W)	2009	Andesite/Basaltic Andesite	Caldera	Vaughan and Webley 2010; Garvin et al. 2018; Global Volcanism Program (Global 2025e); Matoza et al. 2022	ASTER		Not available	No estimate possible
			2014				RapidEye	RapidEye, Planet, WorldView	Garvin et al. 2018	
	Vanuatu Volcanic Arc	Kuwae (16.83°S, 168.52°E)	1971	Basalt/Picro-Basalt, Dacite, Andesite/Basaltic Andesite	Caldera	Global Volcanism Program 2025f				Estimated based on cuboid
	Solomon Volcanic Arc	Kavachi (8.99°S, 157.98°E)	1970	Andesite/Basaltic Andesite, Basalt/Picro-Basalt	Stratovolcano	Global Volcanism Program (Global 2025g)	No satellite data or information from GVP available		Not available	No estimate possible
			1976				Global Volcanism Program 2025 g			Estimated based on mean of half ellipsoid and cuboid
			1978				Global Volcanism Program 2025 g		Not available	No estimate possible
			1991				No satellite data or information from GVP available			
			2002				Global Volcanism Program 2025 g			
	Ogasawara Volcanic Arc	Fukutoku-Okano-Ba (*FOB*) (24.29°N, 141.48°E)	1986	Trachyandesite/Basaltic Trachyandesite	Pyroclastic cone, Tuff ring	Maeno et al. 2022; Fauria et al. 2023; Global Volcanism Program (Global 2025h)	Landsat MSS		Global Volcanism Program (Global 2025h)	Estimated based on cuboid

Table 1 (continued)

Tectonic setting	Tectonic region	Volcano and *abbreviation* (LAT/LON)	Year(s) of island formation (* still existing)	Rocks	Volcano type	Information source of				
						General	Maximum initial island area	Evolution of island area	Height	Volume
			2021				Planet, TerraSAR-X		Global Volcanism Program (Global 2025h), Maeno et al. 2022, Fauria et al. 2023	
		Nishinoshima (*N*) (27.25°N, 140.87°E)	(*1973/74, not part of this study*), 2013*	Andesite/Basaltic Andesite	Caldera, Pyroclastic cone(s)	Maeno et al. 2021; Global Volcanism Program (Global 2025j)	TerraSAR-X	Planet, TerraSAR-X	ALOS World DEM, Airborne 2.5 m DEM (Geospatial Information Authority of Japan GSI (2023))	
		Iwo Jima (27.76°N, 141.33°E)	2023	Trachyandesite/Basaltic Trachyandesite, Trachyte/Trachydacite	Caldera, Tuff cone	Nagai et al. 2025; Global Volcanism Program 2025i	Planet	Planet, TerraSAR-X	Nagai et al. 2025	Estimated based on cone
	Aleutian Volcanic Arc	Bogoslof (53.93°N, 68.03°W)	(*1992, not part of this study*), 2016*	Trachyandesite/Basaltic Trachyandesite, Basalt/Picro-Basalt, Andesite/Basaltic Andesite	Stratovolcano, Lava dome(s)	Waythomas et al. 2020a, b; Coombs et al. 2019; Global Volcanism Program 2025 k	Waythomas et al. 2020a	Planet	IFSAR DEM Intermap Technologies Inc (2018)	

Landsat: https://www.usgs.gov/landsat-missions/landsat-satellite-missions; Sentinel-2: https://www.esa.int/Applications/Observing_the_Earth/Copernicus/Sentinel-2; PlanetScope & RapidEye: https://www.planet.com/; TerraSAR-X: https://www.dlr.de/en/research-and-transfer/projects-and-missions/terrasar-x; TanDEM-X: https://www.dlr.de/en/research-and-transfer/projects-and-missions/tandem-x; WorldView: https://www.euspaceimaging.com/; ASTER: https://terra.nasa.gov/about/terra-instruments/aster

Table 2 Parameters analyzed (Global Volcanism Program = GVP)

#	Parameter	Information source and method	Unit (s)	Accuracy
1	Whether the island still exists. If not, how it got destroyed (erosion or explosion)	Reports from the GVP database, from the literature (if available) and own satellite observations	No unit	High accuracy
2	Approximate date of island formation		Date	Uncertainty up to in the order of weeks for islands formed in the 1960s–1970s; later uncertainty reduced continuously with improved observation frequency by satellites
3	Island lifetime; for islands still existing when writing this manuscript, March 11, 2025, was used as end date to calculate the lifetime		Days	
4	Date and duration of eruption episodes		Date and days	
5	Thermal activity and its duration (for islands formed after the launch of MODIS in December 1999)	Analyzed using MIR band data of MODIS and VIIRS (Schroeder et al. 2014; Giglio et al. 2016), derived from NASA FIRMS (FIRMS 2025). Only nighttime acquisitions were considered to exclude possible false classification of thermal anomalies due to sunglint over the ocean during daytime (Plank et al. 2025). All nighttime hotspots were considered, except for Nishinoshima 2013, where only hotspots with thermal activity > 5 MW were considered for distinguishing the different eruption phases based on the thermal activity. (Lower energetic thermal activity over Nishinoshima 2013 was noted for its entire lifetime)	Days	Data available since early 2000. Observation frequency and detection accuracy increased with the launch of VIIRS (2011; cf. Fig. 2a) For details on detection accuracy see (Schroeder et al. 2014; Giglio et al. 2016)
6	Maximum island area per eruption episode (if more than one) and for entire lifetime	Measured using the satellite data with the highest spatial resolution available. For islands formed prior to regular satellite observations, information from the GVP database and from the literature were used. Some GVP reports provided only information on the island's shape, including diameter or length and width as estimated by observers on board of ships or airplanes. This information was then used to approximate the island's area. (cf. Table 1)	m^2	Depending on the spatial resolution of the available satellite data (ranging from 80 m to < 1 m; cf. Fig. 2a). Higher uncertainty for areas calculated from length measurements and shape information from the GVP
7	Island volume above sea level	Derived from (1) Digital Surface Models (DSMs), (2) differences of DSMs derived from airborne, or satellite data acquired in different years and (3) volumes reported in the GVP database or from the literature (cf. Table 1). In case of missing DSM/volume data: height information (if available) was used to estimate the volume, using simplified equations for a cone, half ellipsoid, cuboid and the mean of the last two (depending on the island's shape)	m^3	Depending on the spatial resolution of the available DSMs and satellite data. (cf. Table 1). Higher uncertainty for estimated volumes. Comparison with DSM based estimates showed at least the same order of magnitude
8	Compactness of the island by calculating shape index *SI* normalized to the area of a circle (Eq. 1)	$SI = \frac{P}{2\sqrt{\pi \cdot A}} \quad (1)$ with island perimeter *P* and island area *A*. This normalization gives the most compact island shape, i.e., a circle, the smallest value of $SI = 1$, while more irregular or elongated islands have an $SI >> 1$	No unit	Depending on the spatial resolution of the available satellite data (ranging from 80 m to < 1 m; cf. Fig. 2a); or airborne data in case of Surtsey

Table 2 (continued)

#	Parameter	Information source and method	Unit (s)	Accuracy
9	Appearance of floating pumice	Visual inspection of Sentinel-2/Landsat imagery; or if these were too cloudy MODIS/VIIRS data were used	No unit	Long-period of cloud coverage influences the accuracy
10	Eruption style, including the Volcano Explosivity Index (VEI)	Based on information reported in the GVP database and literature	No unit	Depending on the detail of the information provided in the reports of the GVP and the literature
11	Material erupted and volcanic landform produced			
12	Percentage of thermal activity (p_{th}): duration of thermal activity (t_{th} #5) as percentage of the island lifetime (t_{life} #3) (Eq. 2)	$p_{th} = \frac{t_{th}}{t_{life}}$ (2)	%	Depending on accuracies of the parameters #3 and #5
13	2D erosion rate (e_{2D}): a) For islands that completely eroded: maximum island area (A_{max} #6) divided by island lifetime (t_{life} #3) (Eq. 3) b) For islands that are still existing: Difference of maximum island area (A_{max} #6) and island area on March 11, 2025 (A_{2025}), divided by island lifetime until March 11, 2025 (t_{life} #3) (Eq. 4)	$e_{2D} = \frac{A_{max}}{t_{life}}$ (3) $e_{2D} = \frac{A_{max} - A_{2025}}{t_{life}}$ (4)	%	Depending on accuracies of the parameters #3 and #6
14	3D erosion rate (e_{3D}): similar to #13, but based on the island volume measurements V (#7) instead of the 2D areal measurements (Eq. 5–6)	$e_{3D} = \frac{V_{max}}{t_{life}}$ (5) $e_{3D} = \frac{V_{max} - V_{2025}}{t_{life}}$ (6)	%	Depending on accuracies of the parameters #3 and #7
15	Percentage of daily erosion: calculated in 2D ($e_{2D,daily}$) and 3D ($e_{3D,daily}$) by dividing the 2D erosion rate (#13) or the 3D erosion rate (#14) by the island area (#6) (Eq. 7) or island volume (#7) (Eq. 8). Note, for islands that completely eroded, #15 is the same as the inversion of the island lifetime (Eq. 9)	$e_{2D,daily} = \frac{e_{2D}}{A_{max}}$ (7) $e_{3D,daily} = \frac{e_{3D}}{V_{max}}$ (8) For completely eroded islands: $e_{2D,daily} = e_{3D,daily} = \frac{1}{t_{life}}$ (9)	%	Depending on accuracies of the parameters #3, #6 and #7
16	Information on the climate, including temperature and precipitation	Derived from (Zepner et al. 2020): https://climatecharts.net/. Data source is the NOAA Global Historical Climatology Network. Climate information was taken from climate station located next to the islands	°C; mm	See Zepner et al. (2020); depending on the distance from the next climate station
17	Information on wave direction during the lifetime of the islands	We used the parameter "mean wave direction" (monthly averaged reanalysis) from the fifth-generation reanalysis data (ERA5) of the European Centre for Medium-Range Weather Forecasts (ECWMF; Hersbach et al. 2020), which are available via the Copernicus Climate Data Store (https://cds.climate.copernicus.eu/). For more details see https://codes.ecmwf.int/grib/param-db/140230. Histogram analysis was performed to identify the main wave direction	degrees	Cf. https://codes.ecmwf.int/grib/param-db/140230

Table 2 (continued)

#	Parameter	Information source and method	Unit (s)	Accuracy
18	Information on wave height during the lifetime of the islands	We used the parameter "significant height of combined wind waves and swell" from the ERA5 data of the ECWMF (Hersbach et al. 2020), which are available via the Copernicus Climate Data Store (https://cds.climate.copernicus.eu/). The "significant height of combined wind waves and swell", represents the average height of the highest third of surface ocean/sea waves generated by wind and swell. This is a common way of summarizing the wave record into a single measure (Holthuijsen 2007). For more details see https://codes.ecmwf.int/grib/param-db/140229. We calculated the cumulative distribution of the wave height observed during the islands' lifetimes. Next, the highest 5% of the wave height observed was derived	m	Wang & Wang, (2021) report a root mean square error of 0.325 m under most typical sea states (0.5 m < significant wave height < 4 m). Fanti et al (2023) compared the ERA5 wave height data against measurements from coastal buoys and found for the 5% of the highest wave height an underestimation of ~ 9% on global average
19	The average wind speed at 10 m height	Derived from the Global Wind Atlas https://globalwindatlas.info, which uses a downscaling process down to 250 m, using as input the atmospheric re-analysis data of the ERA5 dataset from the European Centre for Medium-Range Weather Forecasts (ECMWF) based on the simulation period 2008–2017. For more details see https://globalwindatlas.info/en/about/method	m/s	Cf. https://globalwindatlas.info/en/about/method

Results

Satellite images shown in Fig. 3 document the evolution of selected examples of volcanic islands we analyzed. See Supp-Fig. 1 for the other islands and Supp-Fig. 3 for examples of time series. Quantitative parameters following Table 2 are presented in a series of plots below, and are available in a database format (Supp-Tab. 1).

The relationship between the lifetime (parameter #3) of the newly formed volcanic islands and the maximum island area (parameter #6) after the eruption phase (or phases; cf. Supp-Fig. 2) is shown in Fig. 4. The island of Surtsey has existed since 1963 and accumulated a rather large

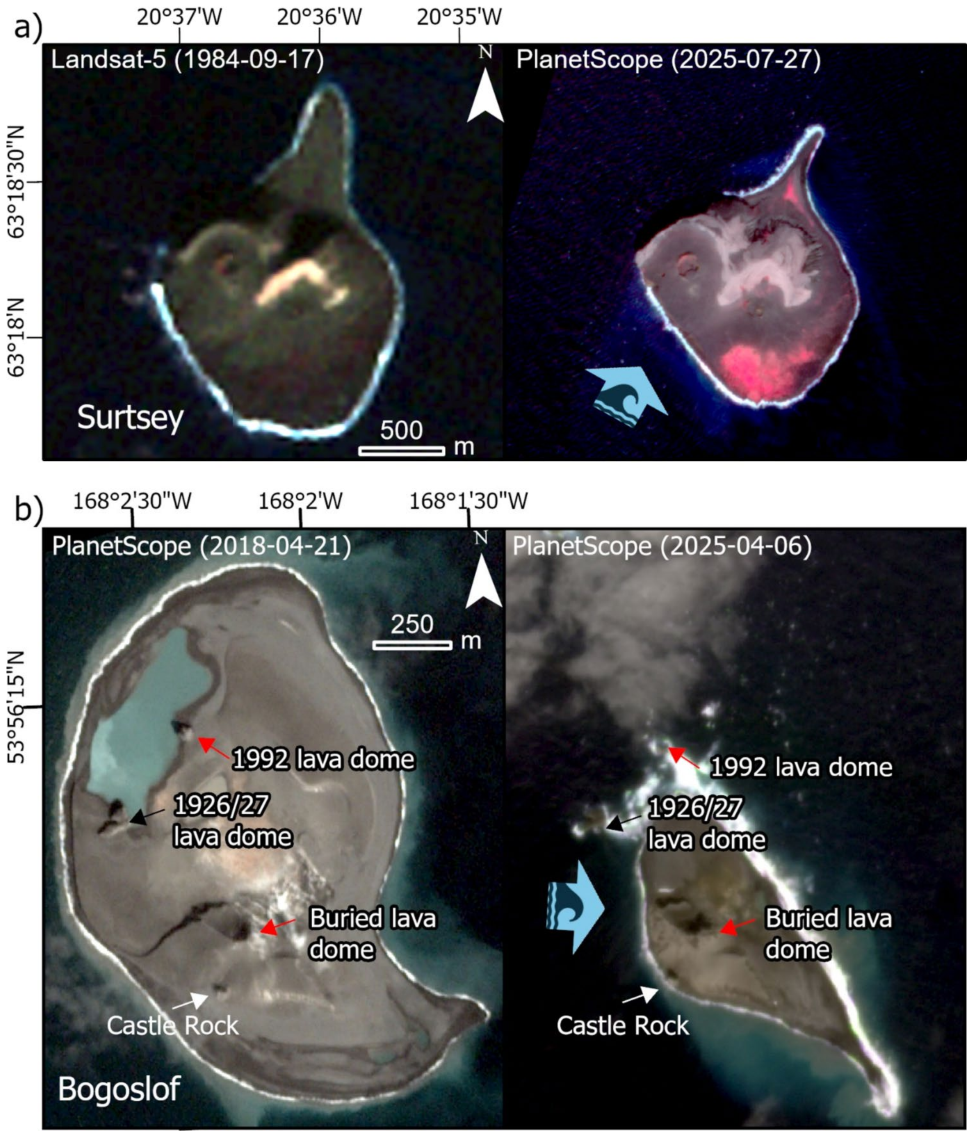

Fig. 3 Examples of satellite images showing the evolution of the analyzed islands. All images per island are shown at the same scale. North arrow and coordinates are only given in the first frame of each sequence. The blue arrow shows the main wave direction for the period of the islands' lifetime (parameter #17) according to the Copernicus Climate Data Store (https://cds.climate.copernicus.eu/). **a**) Example of a long existing island: relatively slow erosion processes on Surtsey 1963 monitored by Landsat 5 in September 1984 (first available HR satellite image after the eruption in 1963) and PlanetScope in July 2025 (false-color representation, living vegetation red), showing a decrease in the land area. **b**) Example of fast erosion processes: Bogoslof 2016 island after the end of the 2016/17 eruption period monitored by PlanetScope (left April 2018, right April 2025). **c**) Example for island growth: Nishinoshima 2013 Island monitored by TerraSAR-X (TSX) in November 2013, November 2014 and April 2025. **d**) Example of island growing, erosion and destruction: Hunga 2014 Island monitored by RapidEye in November 2014 (shortly before the formation of the 2014 island in mid-December 2014) and by WorldView-2 in November 2020, January 2022 and February 2022. The island was almost completely destroyed during an VEI 5 eruption on January 15, 2022

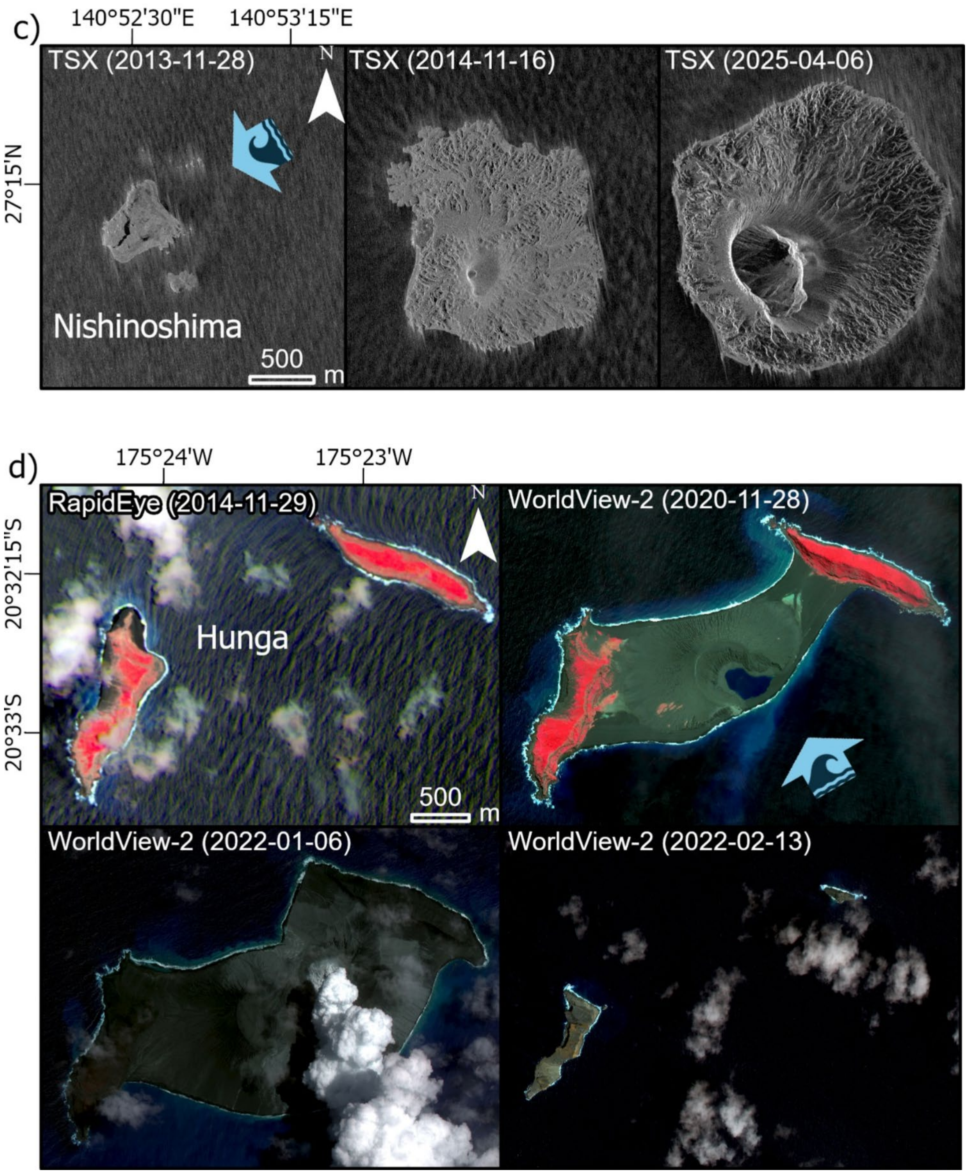

Fig. 3 (continued)

area (2,650,000 m^2). The comparable small Late'iki 1995 island (75,000 m^2) was also characterized by a long lifetime (> 24 years). Other islands of double and even larger areas were eroded more quickly, e.g., Home Reef 1984 and 2006, Fukutoku-Oka-no-Ba 1986 and 2021 had lifetimes of < 1 year. In contrast, Sholan 2011, reached a maximum area between that of Fukutoku-Oka-no-Ba 1986 and Fukutoku-Oka-no-Ba 2021 and persisted for over 7 years. Hunga 2009, on the other hand, despite being 3.6 times larger in area than Sholan, was eroded within only about 400 days. This comparison shows that, in general, the islands' area is not alone the critical factor for a long lifetime.

The islands' material and types of volcanic landforms (parameter #11) are another factor of longevity (Figs. 4, 5, and 6). Volcanic islands formed of unconsolidated tephra (crosses) show short lifetimes of around 100 days or less. Exceptions are the very large Home Reef 2006 and Hunga 2009 islands. Islands formed of lava flows (squares, Home Reef 2022) and lava domes (diamonds, Late'iki 1995) are characterized by much longer lifetimes of several years (or even decades) (cf., hypothesis H5). Kavachi 1978, Iwo Jima 2003 and Nishinoshima 2013 are combinations of different eruption materials and volcanic landforms, with lava flows around a primary formed pyroclastic cone (red-filled triangles). Nishinoshima 2013 grew by continued lava flows over the several years (Fig. 3c).

We also consider the initial island volume (parameter #7) in comparison with the islands' lifetime (parameter #3)

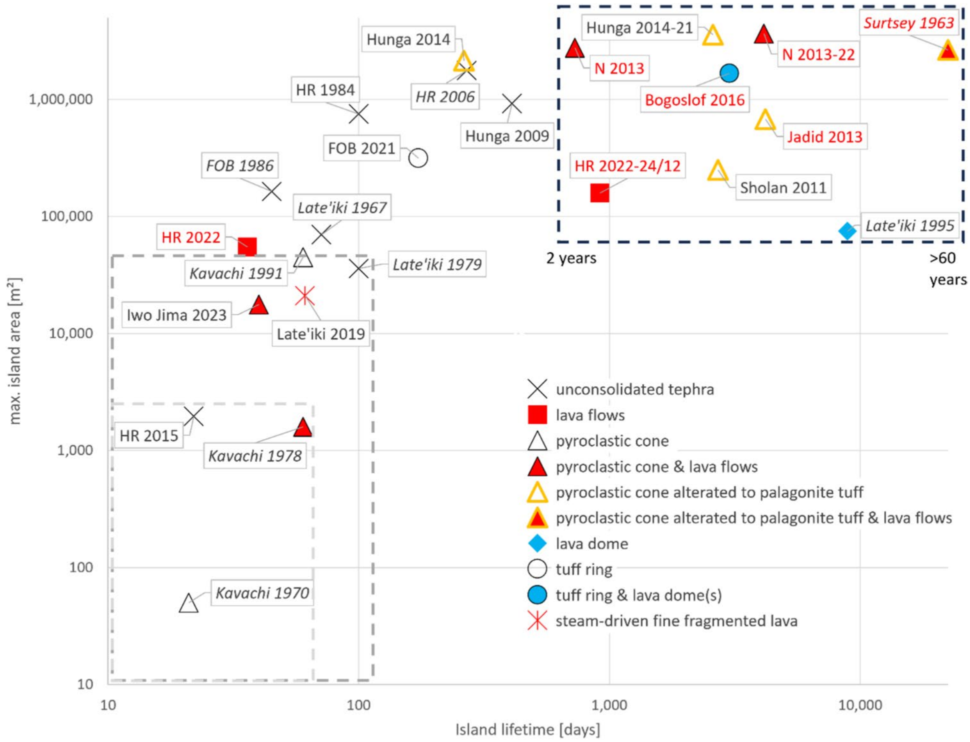

Fig. 4 Island lifetime vs. maximum (max.) initial island area shown in log–log scale for 21 islands for which information about the area could be derived (cf. Table 1). For the growing islands Home Reef (HR), Nishinoshima (N) and Hunga, one additional area measurement for each island at a later stage is shown (cf. Supp-Fig. 2 for a more detailed timeline). FOB = Fukutoku-Oka-no-Ba. Islands still existing (red letters), islands eroded (black letters). Information on initial maximum island area from the Global Volcanism Project (2025) database (italic text) having a higher uncertainty (except for Surtsey, which is based on airborne measurements) than the area information derived from satellite data (normal text). Table 1 lists which satellite data were used for which island. Cf. Figure 2a for their spatial resolution, which determines the uncertainty of the area measurements. The uncertainty values are too small to be readable in log–log scale. Symbols represent the material/volcanic landform. Light gray box: islands with areas < 2,000 m^2 and lifetimes < 2 months; dark gray box: islands with areas < 50,000 m^2 . and lifetimes < ~100 days (cf. "Discussion of hypotheses" section, hypothesis H1); black box: long-lived islands of hard material (cf. hypothesis H5)

(Fig. 5). Note that no volume information was available for five volcanic islands.

The result resembles the area-based analysis. The more voluminous islands Surtsey and Nishinoshima 2013 have a long lifetime, followed by Jadid 2013, but larger volume does not guarantee a longer lifetime (compare, e.g., Home Reef 2006 to Late'iki 1995).

Further, a qualitative ranking of the islands' material (parameter #11), ranging from unconsolidated tephra to hard lava flows and domes, is compared with the islands' lifetime (parameter #3). The black box in Fig. 6 shows a clear clustering of the long-lived islands, mainly formed of hard material such as lava flows or palagonite tuff. Also, the islands formed of unconsolidated tephra show a strong clustering at shorter lifetimes (gray box in Fig. 6). Exceptions are Iwo Jima 2023, Kavachi 1978 and Bogoslof 2016. The first two formed pyroclastic cones and in addition small lava flows, but these islands were too small to exist longer (cf. Fig. 4 and "Discussion of hypotheses" section , hypothesis H1). Bogoslof, on the other hand, formed a very large island mainly built of tuff rings, i.e., easily erodible unconsolidated material, as well as including four smaller lava domes formed of consolidated material that erodes slower (Figs. 3b, 4; cf., "Discussion of hypotheses" section, hypothesis H5).

Comparison of the normalized shape index *SI* (cf. Equation 1, parameter #8) after the end of the initial eruption phase with the daily erosion rates (as percentage of the entire island area, parameter #15) is shown in Fig. 7. The initial Home Reef 2022 shows an $SI = 1.03$, closely resembling a circle (Supp-Fig. 1k), followed by Late'iki 1995 (Supp-Fig. 1b) and Sholan 2011, Surtsey 1963, Jadid 2013 and Bogoslof 2016 all having an $SI \sim 1.10$. All these compact islands are characterized by a relatively low erosion rate compared to the irregular or elongated shaped islands ($SI >> 1$) like Iwo Jima 2023 and Fukutoku-Oka-no-Ba 2021. An exception is the very small and very short-lived Home Reef 2015 island, an island that we newly detected by analyzing time series of RapidEye data (cf. Fig. 4, "Discussion of hypotheses" section, hypothesis H1). As initially two islands were formed during the eruption of

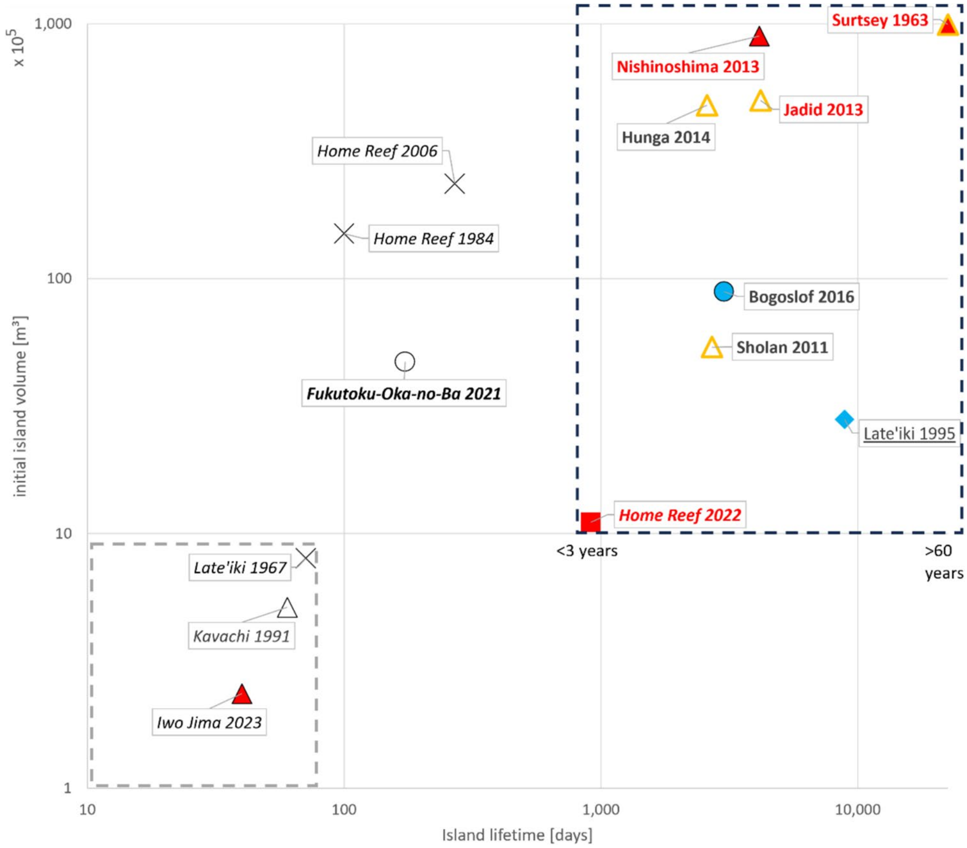

Fig. 5 Island lifetime vs. initial island volume (in × 10.⁵) in log–log scale for 14 islands for which information about the volume was available (cf. Table 1). Volume measurements based on precise Digital Surface Models (DSMs) (bold), based on precise area measurements plus height information (italic and bold), based on volume estimates reported in the Global Volcanism Program (2025a) database (underlined), estimated based on area and height information reported in the Global Volcanism Program (2025 a) database (italic, cf. Table 1). Symbols represent the material/volcanic landform (cf. Fig. 4). Gray box: short-lived islands of small volumes (cf. "Discussion of hypotheses" section, hypothesis H1); black box: long-lived islands of hard material (cf. hypothesis H5)

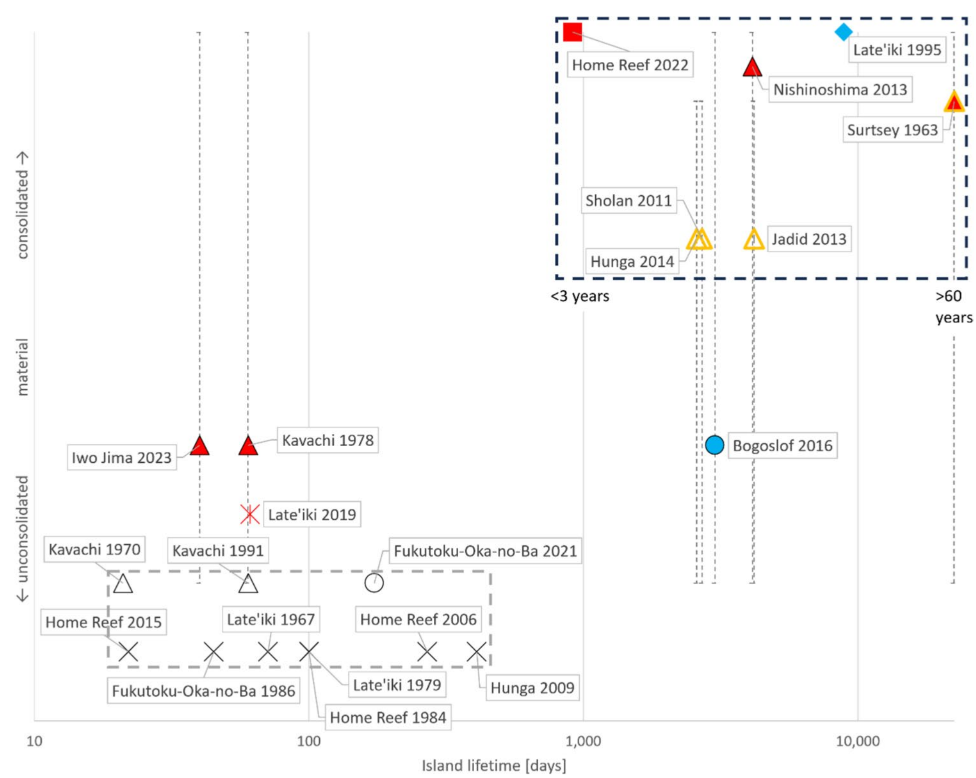

Fig. 6 Island lifetime (in log scale) vs. qualitative ranking of the island material for 21 islands for which information about the erupted material was available. The material ranges from unconsolidated tephra to lava flows and domes. Symbols represent the material/volcanic landform (cf. Fig. 4). The percentage of lava and of pyroclastic material was considered for islands formed of different materials (e.g., a pyroclastic cone and later lava flows). Thereby, the outside of the island was weighted higher. "Error bars" represent the variability of all material of "mixed-material" islands. Gray box: short-lived islands of unconsolidated material; black box: long-lived islands of hard material (cf. hypothesis H5)

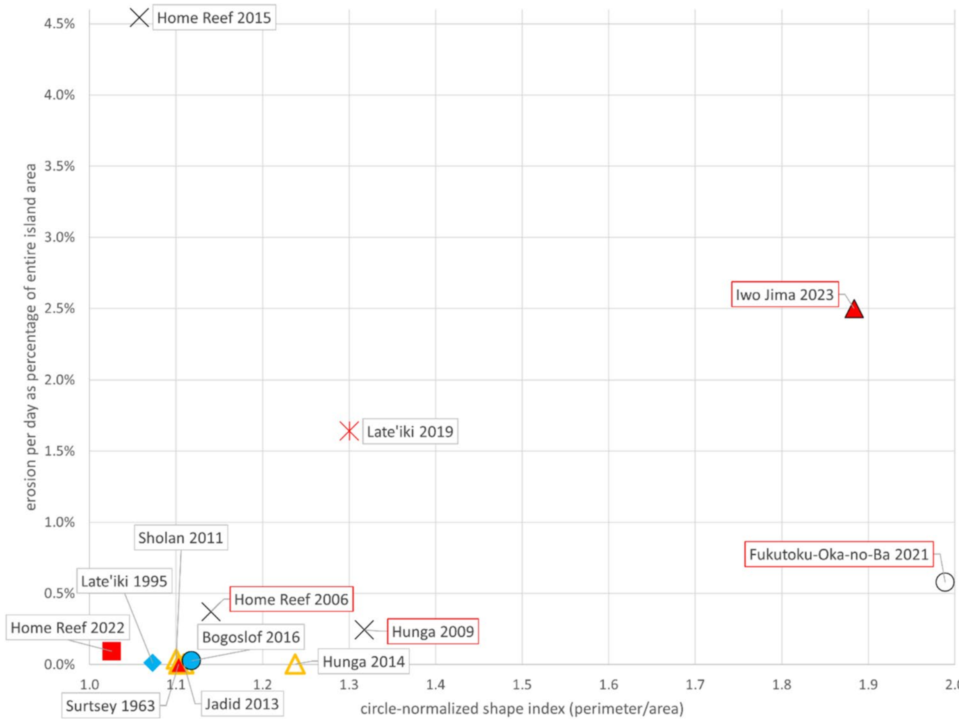

Fig. 7 Circle-normalized shape index (SI) of island perimeter and area (cf. Equation (1)) vs. daily erosion as percentage of the entire island area for 13 islands for which satellite data and or topographic maps were available to derive SI. Symbols represent the material/volcanic landform (cf. Fig. 4). Red boxes show eruptions with floating pumice observed

Fukutoku-Oka-no-Ba 2021 (Supp-Fig. 1j), this island is characterized by a very high *SI* value.

For islands with available volume/volume change information, a volumetric erosion rate was calculated. For all islands that completely eroded, parameter #15 is the inverse of the island's lifetime (parameter #3) and therefore independent of an area or volume-based analysis. For still existing islands, the parameter #15 values of area and volume-based analysis are similar (maximum difference < 0.05%).

Figure 8 compares the eruption duration (parameter #4) with the islands' lifetime (parameter #3) and additionally shows information on the VEI (parameter #10) and whether floating pumice (#9) was observed during the eruption. Islands with longer lifetimes are mainly characterized by a longer duration of the initial eruption phase. Surtsey 1963 has by far the longest lifetime and eruption duration, followed by Nishinoshima 2013 and Bogoslof 2016. Sholan 2011 and Late'iki 1995 had long lifetimes of several years or even decades but were characterized by much shorter eruption durations (25 or 19 days). The short-lived islands at Kavachi Volcano as well as Iwo Jima 2023, Late'iki 1967 & 2019 were all characterized by eruption durations of < 45 days.

Except for Iwo Jima 2023, the other four eruptions that produced floating pumice (red in Fig. 8) had short eruption durations. The pumiceous eruptions formed islands with a relatively high daily erosion rate (Fig. 7) and short lifetime.

Most island-forming eruptions were classified as VEI 2, followed by VEI 3 and VEI 1. Only Fukutoku-Oka-no-Ba 2021 was a VEI 4.

For islands that formed after the year 2000, Fig. 9 shows thermal volcanic activity detected by MODIS and/or VIIRS (parameter #12) as a percentage of the entire lifetime (parameter #3). Except for Kavachi 2002, where no thermal anomalies were detected by MODIS, for all other 11 islands that formed after the launch of MODIS in December 1999, thermal activity was detected. The highest thermal percentage value (50%) was registered for Iwo Jima 2023. For islands with lifetimes longer than 100 days, the amount of thermal activity shows a clear separation between effusive and explosive volcanism (cf. "Discussion of hypotheses" section, hypothesis H5).

To investigate the influence of the environmental conditions on the islands' lifetime, we analyzed climate observations taken from the closest climate station (see Supp-Fig. 4; Table 2, parameter #16). Surtsey and Bogoslof are characterized by a subpolar oceanic climate (Cfc), Jadid and Sholan by a hot desert climate (BWh), Kavachi, Fukutoku-Oka-no-Ba, Nishinoshima and Iwo Jima by a tropical monsoon climate (Am), Kuwae, Home Reef, Late'iki and Hunga by a tropical rainforest climate (Af).

Waythomas et al. (2010) discuss for Kasatochi Island (Aleutian Arc), the strong erosional effects that large storms have on the unconsolidated material erupted during the 2008 eruption. The same material dominated during the 2016/17 Bogoslof eruption. Therefore, we selected Bogoslof as an

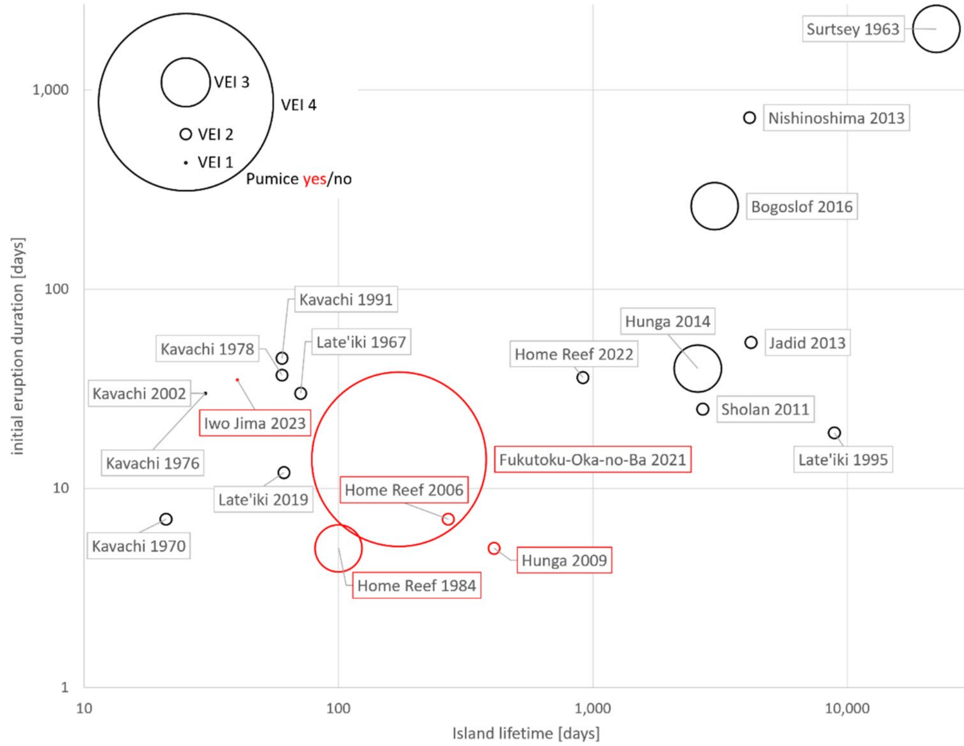

Fig. 8 Island lifetime vs. initial eruption duration in log–log scale for 20 islands for which information on the eruption duration was available. The circle size marks the Volcano Explosivity Index (VEI). Red circles and boxes show eruptions with floating pumice observed

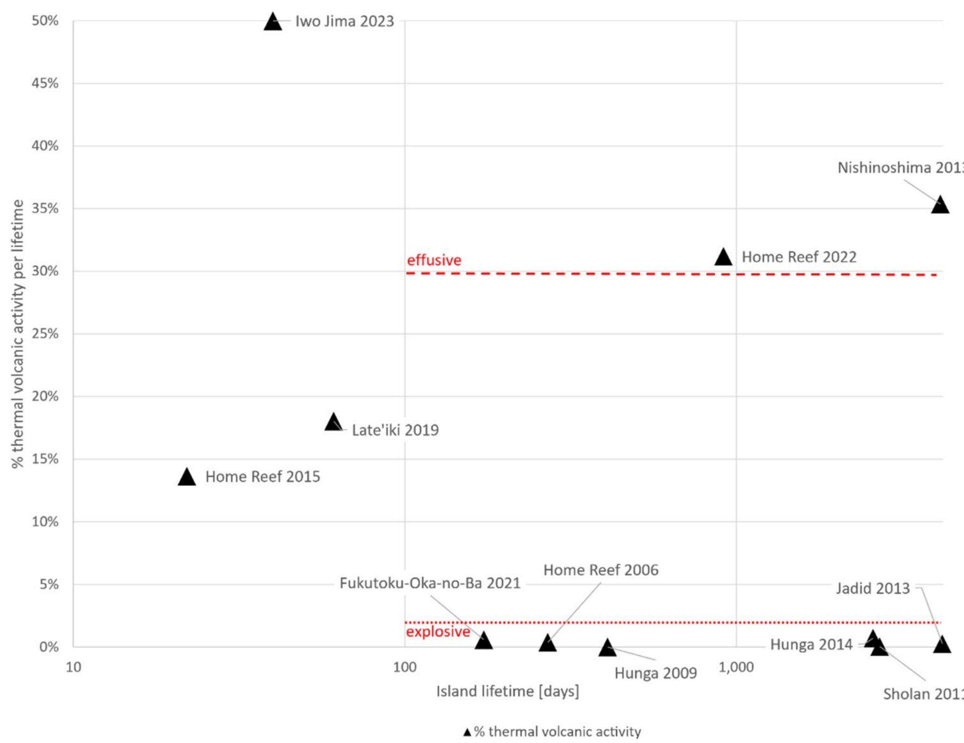

Fig. 9 Percentage of thermal volcanic activity in relationship to the entire lifetime of the volcanic island (in log-scale) for 11 islands which were formed after the year 2000 (launch of MODIS December 1999). Islands with lifetimes longer than 100 days could be separated into islands with low percentage thermal activity – typical for explosive volcanism (below the red-dotted line) – and islands with high percentage thermal activity – typical for effusive volcanism (above the red-dashed line)

example to show the strong erosional effect of large storm waves (Supp-Fig. 6).

Supp-Fig. 5 reports the cumulative distribution of the wave height observed during the periods of the islands' lifetimes (based on parameter #18). In order to consider the strong erosional effect of storms, we derived for each island the highest 5% of the wave height from the cumulative distribution. Surtsey has the harshest environmental conditions with a highest-5% wave height larger than 5.5 m (maximum up to 11.6 m) as well as average wind speeds of 9.9 m/s (parameter #19, see Supp-Fig. 3). This is followed by Bogoslof and Fukutoku-Oka-no-Ba. Home Reef, Late'iki and Hunga have similar wave height distributions (Supp-Fig. 5) and highest-5% wave heights of 2.6 to 2.8 m, followed by Iwo Jima and Kavachi. Kuwae, Sholan and Jadid show the lowest values. As the average wind speeds are with the exception of the high wind speed locations Surtsey and Bogoslof very similar (~6.1 m/s) for the other islands (cf. Supp-Fig. 4), we focus on the highest-5% wave heights (parameter #18) for the period of the islands' lifetime and compare this parameter with the observed erosion rates (parameter #15) (Fig. 10).

Discussion

This study offers a systematic remote sensing analysis of how young volcanic islands persist and erode over time. For a set of 24 islands, we integrated up to four decades of multi-sensor satellite observations with data from the Global Volcanism Program and published studies. Assessing island lifetime, shape, area, volume, and their temporal evolution allowed us to evaluate eight hypotheses, which are discussed below after laying out the limitations of this study. Further, the correlation between the different parameters was analyzed. In addition, based on our eight hypotheses, we used timeseries analysis of satellite data of individual islands and comparative studies between different islands of the same physical characteristics to roughly project the expected lifetimes of the existing volcanic islands Home Reef, Bogoslof, Jadid, Surtsey, and Nishinoshima (cf. Supplementary 6, Supp-Tab. 3).

Limitations

The following limitations must be considered for the presented study. For "older" islands (formed 1960s–1980s) no satellite observations were available. Visual observations from ships or airplanes have a higher uncertainty regarding the length, width, area, and height of an island. Compared to modern VHR satellite images, such observations are generally less frequently available, especially in remote areas. Therefore, for these "older" islands the absolute values have to be taken with caution. The problem with sparse temporal sampling and ground-based estimates of island areas is illustrated, for example, by the Home Reef formation in August 2006. Initially, an area of ca. 1.770.000 m^2 was reported (Global Volcanism Program 2025c). However, two months later the first available high-resolution satellite image by ASTER showed an area of ca. 260.680 m^2 (cf. Supp-Fig. 2). Because unconsolidated tephra was reported as material for this island, fast erosion is highly likely. However, the daily erosion rate would have been 1.5%, substantially higher for the first 2 months compared to the $< 0.4\%$ since then. Thus, we have to consider that the original area might have been overestimated. An exception for these early years is the well-documented evolution of the island of Surtsey, due to its proximity to mainland Iceland, duration of the eruption, and

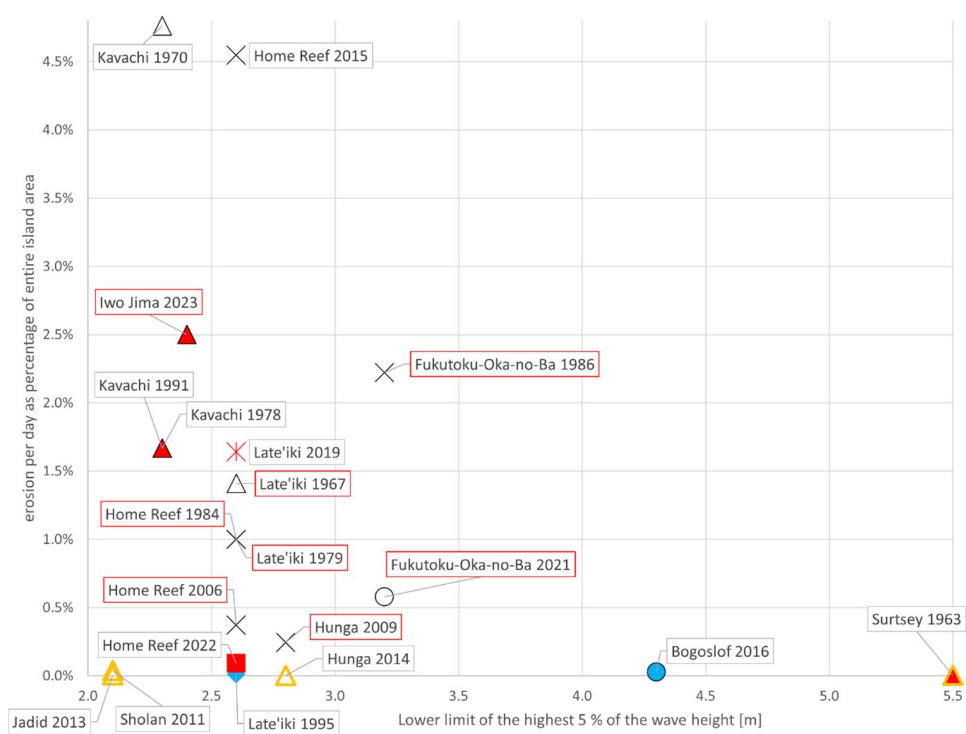

Fig. 10 Lower limit of the highest-5% of the wave height during island lifetimes vs. daily erosion as percentage of the entire island area (cf. Fig. 7) for 20 islands for which information about the area and its change over time was available (cf. Table 1). Symbols represent the material/volcanic landform (cf. Fig. 4). Red boxes show eruptions with floating pumice observed

keen observations of local volcanologists. Further, the lower observation frequency of remote regions was also true during the early days of the satellite era (1980s–1990s) as the first satellites with suitable spatial resolution did not cover the entire globe (cf. "Satellite observations for monitoring newly formed volcanic islands" section).

For the analysis of the formation of temporary beaches (hypothesis H7) and of detailed structures on the islands' surface, VHR data are necessary. While these datasets have been available since the early 2000s, they mostly come from commercial satellites that require tasking and lack systematic global coverage. The PlanetScope constellation is an exception, though its 3 m spatial resolution is not sufficient for detailed analysis. It therefore remains a challenge to task image acquisitions so that satellite data is systematically available for monitoring of a newly formed island (cf. Home Reef 2022; Plank et al. 2025).

Regular and systematic 3D information, required for volumetric analysis is available but limited with current satellite systems. Table 1 provides more details on area and volume measurements/estimates for each island investigated. Closing this data gap in the future will require planned tasking of VHR optical stereo data to be realized promptly with the formation of new volcanic islands for detailed documentation of their fast and dynamic evolution. A limitation remains that these data are currently only available commercially, and they rely on clear-sky conditions. Harmony (Pappas et al. 2025), a passive SAR sensor planned to fly in bi-static constellation with Sentinel-1 in order to generate DSMs more regularly than the existing TanDEM-X mission, will be a great improvement.

Due to the remote location and sometimes short-lived phenomena, detailed petrological reports are rare and mostly available only for Surtsey and Bogoslof. Analysis of samples collected via an autonomous underwater vehicle after the erosion of the Late'iki 2019 island (Yeo et al. 2022), is an exception for such a remote location.

Lastly, we have to consider that our study relies on information derived from satellite data, supported by information from the literature and the Global Volcanism Program database, with few direct observations. Our sample size is relatively small and includes varied conditions, making it difficult to draw broad conclusions (cf. "Correlation between investigated parameters" section). However, our synthesis provides high-level insights and trends about the evolution of volcanic islands based on their settings.

Discussion of hypotheses

We use our database of volcanic island observations to assess the hypotheses put forward in "The hypotheses" section.

H1: The larger the initial island the longer is the lifetime of an island In general, the larger an island, the longer time is required by ocean waves to erode it. The largest one – considering the initial size—of our investigated volcano islands, Surtsey, has the longest lifetime. However, Late'iki 1995 was 35 times smaller and remained intact for 24 years while other islands of twice or more its area were eroded within less than a year. As shown in Figs. 4 and 5, which compare the lifetime of the islands with their areas and volumes, we can conclude that larger islands do not always live longer.

The material that comprises the island is a key parameter that determines the island's lifetime. However, when looking at the smaller islands, we see that a minimum island size is necessary to withstand erosion from ocean waves and to remain intact for some time. The very short-lived islands Home Reef 2015, Kavachi 1970 & 1978 (1–2 months) were < 2000 m^2—too small to remain intact longer (cf. light gray box in Fig. 4). Even Late'iki 2019, Iwo Jima 2023 and Kavachi 1991, which were one order of magnitude larger in area still had lifetimes of < 2 months. Most of these islands were formed of tephra (cones), but on Kavachi 1978 and Iwo Jima 2023 small lava flows were observed. Thus, these islands were at least partly formed of hard material, but their initial size was too small to remain intact longer than 2 months. Independent of the material, our comparison of area vs. lifetime suggests that a minimum initial area of around 50,000 m^2 might be a reasonable threshold to give the island a chance to exist longer (cf. dark gray box in Fig. 4). Just above this threshold lies the initial area of Home Reef 2022, an island that remained intact 1 year until it was further expanded in subsequent eruption phases (Supp-Fig. 1k, Supp-Fig. 2, Plank et al. 2025). However, it has to be considered that Home Reef 2022 is fully formed of lava flows, making its lifetime perhaps an upper limit for this island size.

The island's height is another critical factor in withstanding erosion. Following Nunn (1994), a certain minimum volume produced at a certain eruption rate is needed so that a new island can form. Thus, we also estimate a minimum volumetric threshold. The three short-lived islands with height information had small volumes: Iwo Jima 2023, Late'iki 1967, and Kavachi 1991. The estimated minimum volumetric threshold based on our results thus lies between these islands (Late'iki 1967 ~ 800,000 m^3; cf. gray box in Fig. 4) and the initial volume of Home Reef 2022 (~ 1,100,000 m^3).

H2: Due to shorter coastline length, compact circular islands withstand erosion better than irregular islands The comparison of the *SI* value after the end of the initial eruption phase with the daily erosion rates (Fig. 7) suggests that all compact-shaped islands (low *SI* values), are characterized by low daily percentage erosion rates (< 0.1%), i.e., a long lifetime. In contrast, irregular or elongated-shaped islands

($SI >> 1$), like Iwo Jima 2023 and Fukutoku-Oka-no-Ba 2021, are characterized by a higher erosion rate (and therefore shorter lifetime). However, this has to be considered with caution. First, the high erosion rate of Iwo Jima 2023 is due to its very small area (Fig. 4), like Home Reef 2015 (cf. hypothesis H1). This leaves Fukutoku-Oka-no-Ba 2021 as the only example for an island with a high SI value to be compared with the ones with a lower SI value. From the few samples we have for this analysis, we cannot determine the influence that the island's shape has on its lifetime.

H3: Islands formed during long-lasting eruptions have a longer lifetime In Fig. 8 the initial eruption duration is compared with the island's lifetime. In general, it seems that a long eruption duration supports a longer island lifetime, as shown by Surtsey 1963, with by far the longest lifetime and eruption duration (> 3 years), followed by Nishinoshima 2013 and Bogoslof 2016. This is confirmed by a significant positive correlation between eruption duration and island lifetime ($r = 0.85$, $p = 1.08 \times 10^{-6} < 0.05$; cf. Supp-Table 2). However, with Sholan 2011 and Late'iki 1995, there are islands with a relatively short eruption duration, but a long lifetime, i.e., the material of which the island is formed seems to be more important.

H4: Islands that grew during several eruptive episodes have a longer lifetime During an eruptive episode, an island can compensate for the lost land that was eroded since the end of the previous eruption episode. Short response periods of a volcano and further growth can even enlarge the island to give it a higher chance to remain intact until the beginning of the next eruption episode. The still growing island Home Reef 2022 (Supp-Fig. 1k) and the long-lived Nishinoshima 2013 island, grown during different effusive lava flow eruption episodes (Fig. 3c), are good examples for this process. As both islands are still in their growing phases, it is difficult to compare their final lifetime with other islands that had only one eruption episode. This aspect could be investigated further in future studies. However, renewed volcanic activity can also be destructive. For instance, after renewed activity from November 2021 onwards, Hunga 2014 expanded very fast (Fig. 3d), but shortly after was destroyed by a VEI 5 eruption on January 15, 2022 (Matoza et al. 2022). The much less intensive eruption of Late'iki in October 2019 destroyed the remnants of the 1995 lava dome island and formed the short-lived island Late'iki 2019 (Plank et al. 2020). Renewed activity may also increase the likelihood of tsunamigenic flank or dome collapses, as was the case on Anak Krakatau in 2018 (Walter et al. 2019), on Kadovar in 2018 (Plank et al. 2019) or for some of the dome collapse events on Augustine (Begét and Kienle 1992).

H5: The eruption style and products determine the island's lifetime Figs. 4, 5, 6, and 7 show that the erupted material is the most critical factor impacting the lifetime and the erosion rate of a volcanic island. We divided our analysis between islands built of unconsolidated pyroclastic material, which is easily erodible by ocean waves, versus lava flows/domes, which are more resistant to ocean wave erosion (Nunn 1994). All islands formed of lava domes and lava flows, such as Late'iki 1995 and Home Reef 2022 and at a later development stage Surtsey 1963 and Nishinoshima 2013, have longer lifetimes of several years or even decades (cf. black boxes in Figs. 4, 5, and 6). In contrast, islands built of unconsolidated pyroclastic material had a shorter lifetime of weeks to months except for later-stage hydrothermal alteration (cf. hypothesis H6). Like Surtsey 1963, layers of lava mantled the pyroclastic cone of Nishinoshima 2013 after pyroclastic material had built up a barrier between the eruptive vent and the ocean, and effusive lava flows were erupted that expanded the island and protected it from erosion (cf.) (Maeno et al. 2021). Fukutoku-Oka-no-Ba 2021 and Bogoslof 2016 were both formed of tuff ring(s), i.e., unconsolidated material. While the first one eroded within less than half a year, the latter still exists after several years. Besides being over five times larger than Fukutoku-Oka-no-Ba 2021, during the formation of Bogoslof 2016, also one cryptodome was emplaced. In addition, Bogoslof 2016 was an expansion of an already existing island including three lava domes formed in the past (last eruption in 1992; Waythomas et al. 2020a). Hard rock formed by lava flows or lava domes can withstand erosion from waves over decades to centuries, while the unconsolidated deposits get eroded rather fast, leaving behind the lava dome. For example, Fire Island, formed during an eruption in 1883, was once a lava dome surrounded by unconsolidated eruptive material and is now a sea stack located north of Bogoslof Island (Waythomas et al. 2020b).

The percentage of thermal activity during the lifetime of an island gives information about the eruption style being effusive or explosive. Low thermal percentage values of < 1% indicate short thermal events and are typical for explosive activity (cf. red-dotted line in Fig. 9) as was the case for Fukutoku-Oka-no-Ba 2021 (as confirmed also by the analysis of time series of HIMAWARI data, cf. Supp-Fig. 7) (Maeno et al. 2022; Fauria et al. 2023), Hunga 2009 & 2014 (Garvin et al. 2018), Sholan 2011 and Jadid 2013 (Xu et al. 2015). With thermal percentages of > 30% (cf. red-dashed line in Fig. 8), Home Reef 2022 and Nishinoshima 2013 show greater thermal activity during different periods of their lifetime, typical for effusive eruptions. These two islands also have longer lifetimes. An exception is the short-lived Iwo Jima 2023, that shows the highest thermal percentage values but has a small footprint and thus remained not long (cf. hypothesis H1). However, we cannot conclude that islands formed by explosive eruptions always have a short lifetime. Hunga 2014, Sholan 2011, and Jadid 2013 are examples of long-lived islands initially formed by explosive activity (cf. hypothesis H6).

All eruptions, where pumiceous pyroclastic products were generated, formed islands characterized by high erosion rates and a relatively short lifetimes (Figs. 7, 8, and 10). The occurrence of pumice is indicative of explosive eruptive activity (Bryan et al. 2004) producing fragmented material that is easier to erode (unless welded), which negatively impacts an island's lifetime.

Analysis of the VEI value does not show any relationship to island lifetime (Fig. 8). Fukutoku-Oka-no-Ba 2021, the only VEI 4 eruption, was short-lived, but other islands with much lower VEI were also short-lived.

H6: Hydrothermal alteration of unconsolidated pyroclastic material to palagonite tuff increases islands' resistance to wave erosion This process is well described for Surtsey (Prause et al. 2022), where low temperature hydrothermal activity caused previously unconsolidated tephra to alter to palagonite tuff, which is very resistant to ocean wave erosion. The process of palagonitization was first described 2 years after the end of the eruption phase (Jakobsson 1972). This process may be fast and happen in days to weeks, otherwise Surtsey would not have survived the winter storms. Jakobsson (1972, 1978) reported that the degree of palagonitization was about 64% of the total tephra mass within 10 years, which increased to about 80–85% by 1998 (Jakobsson et al. 2000).

Gravin et al. (2018) assume similar processes for Hunga 2014, also an island with a longer expected lifetime (based on the measured erosion rate). Similar alteration processes as on Surtsey were described by Xu et al. (2015) for the older Zubair islands in the neighborhood of Sholan and Jadid, for which the authors expected similar alteration processes. Our analysis is based on satellite data only; detailed geochemical data of Sholan or Jadid (besides the general information on the rock types, dominantly basalt, as reported in Table 1) were not available. The process of palagonitization is chemically controlled. It has been observed on glassy volcanic ash of basaltic composition (Prause et al. 2022) but not on rhyolitic glass. We can confirm that Sholan and Jadid are both long-lived islands, with similar low daily percentage erosion rates such as Hunga 2014 and Surtsey (Fig. 7). Therefore, we can assume that similar alteration processes of the previously unconsolidated tephra may have started also on Sholan and Jadid.

When exposed to the surface, hydrothermal deposits in general can be mapped using multispectral satellite data (e.g., Gao et al. 2025). Hyperspectral data enable more detailed analysis. However, a feasibility analysis of the possibility to map the surface extension of potential palagonite tuff on the still existing Jadid Island could be a topic of future research when more hyperspectral data, from, e.g., the EnMAP mission, will be available—also over small islands located in remote areas.

All islands where alteration to palagonite tuff was reported had lifetimes of several years, like those islands formed of lava flows and lava domes (cf. black boxes in Figs. 4, 5, and 6). Consequently, for islands originally formed of unconsolidated tephra, hydrothermal alteration to palagonite tuff is a key factor influencing the longevity of the island.

H7: Islands protected by already existing neighboring islands or by accumulated sediments have a longer lifetime Several islands showed the development of "beaches", i.e., material that eroded from the islands and then accumulated on certain sides of the islands. Examples are Surtsey, where a "beach" developed on the northeastern side during the 1970 s (Fig. 3a, Romagnoli and Jakobsson 2015); Home Reef 2022, with up to 100 m wide beaches that developed west and north of the lava flow island (Supp-Fig. 1k); and Jadid, where sediments eroded from the island developed a sand bank towards the southeast, which formed a land bridge to the neighboring island of Saba from April 2019 onwards (Supp-Fig. 1i).

The main wave direction determines where the main erosion happens. As confirmed by oceanographic studies, Surtsey is characterized by a prevailing southwestern direction of coastal waves (Romagnoli and Jakobsson 2015), causing the main erosion to occur on the western and southern side of the island (Óskarsson et al. 2020) and the aforementioned accumulation of sediments on the northeastern side. In case of Home Reef, the main wave direction is from the southeast (Supp-Fig. 1k), which matches well with main erosion on this side of the island (Plank et al. 2025) and the accumulation of sediments on the western and northern side. Sholan 2011, located only 8 km northwest of Jadid 2013, shows a strong seasonal dependency where the sediments form beaches. Varying wind and ocean current directions form beaches on the south of the island during summer and transport the sediments towards the northern side of the island during winter (Xu et al. 2015, Supp-Fig. 1g). This seasonal variation of the accumulated sediments could not be observed on Jadid 2013, where the aforementioned land bridge grew over the years towards the southeast (Supp-Fig. 1i). One reason for this might be that this land bridge is protected by the much larger neighboring island Saba, which is only 1 km away from the southeast of Jadid.

Further, the shape of the island is important. Lava flows (island growing) and erosion processes formed a bay on the western side of Home Reef in 2023 (Supp-Fig. 1k), where sediments accumulated.

In addition, shallow waters and smooth bathymetric relief are required so that sediments can form "beaches", as is the case on the northern side of Surtsey (cf. bathymetry map in Romagnoli and Jakobsson 2015). For Home Reef there is no detailed bathymetry information available. However, overlaying the footprints of the islands formed by the Home Reef Volcano shows that the Home Reef 2006 island covered a much larger area which also extended further to the north and west than the footprint of the island formed in 2022 onwards (Plank et al. 2025). According to observations in November 2008, the remnants of Home Reef 2006 were only about 9–10 m below sea level (Global Volcanism Program 2025c).

Hunga 2014 grew between two already existing islands Hunga Tonga and Hunga Ha'apai. Accumulated sediments connected the new cone with the older islands (Garvin et al. 2018). The cone was therefore protected against erosion on the northeastern and southwestern side. However, the main wave direction at Hunga is from the southeast (Fig. 3d). An island formed in 2009 at the same volcano (Hunga 2009) was eroded rather quickly (within about ~400 days). It was a peninsula, located on the southern side of the already existing island Hunga Ha'apai (Supp-Fig. 1f). As the main wave direction at Hunga is from the southeast, Hunga Ha'apai island could not work as breakwater for the new peninsula.

We can conclude, that hypothesis H7 cannot be confirmed. Accumulated sediments or already existing islands do not necessarily protect an island from erosion; the sediments are rather a consequence of low erosion on a certain side of the island, which is controlled by the main wave (and wind) direction and the local bathymetry. However, as exemplary shown for the post-eruptive development of Kasatochi Island after the 7–8 August 2008; in the case of the development of wider long-term stable beach, these beaches can work as a buffer zone between the wave erosion and the remnants of the original island (Waythomas et al. 2010). Only during large storm events (cf. hypothesis H8) high storm waves can reach and erode the original island on the side of beach location. Further, sediments eroded from the island due to intensive precipitation can accumulate on these beaches (Waythomas et al. 2010).

H8: The environmental conditions, height of sea waves and wind, etc. influence the islands' lifetime Fig. 10 shows the highest-5% of the wave height during the islands' lifetime (derived from the cumulative wave height distribution, Supp-Fig. 5) and compares it to the daily erosion rates. Sholan 2011 and Jadid 2013 have the lowest value of the highest-5% of the wave height and also very low daily percentage erosion rates. But similar low daily percentage erosion rates were observed on Surtsey, the location with the harshest environmental conditions and highest wave heights. Furthermore, the Home Reef, Late'iki and Kavachi volcanoes formed islands several times during the last decades. While their cumulative wave height distribution and the highest-5% of the wave heights for the single volcano locations were stable over time, strong differences in erosion rates were observed. During the formation of a new island, as long as magma interacts directly with ocean water in the hydroexplosive zone (Nunn 1994), unconsolidated pyroclastic material is being erupted. In this phase, the environmental conditions, especially the wave height, are important for whether the island can "survive" the initial phase or not. However, Fig. 10 shows that in the long term the material, of which the island is formed, is more critical regarding the average erosion rate than the wave height. But, assuming the same island volume, eruption rate, material, etc., the location, where an island is formed, and its environmental conditions, especially the wave height and the occurrence of storms, (e.g., North Atlantic vs. Red Sea) would make a strong difference. The larger the wave, the more energy expended, resulting in more geomorphic changes. Supp-Fig. 6 exemplary shows for Bogoslof the strong erosion effects of large waves.

Correlation between investigated parameters

Not all parameters that influence the islands' lifetime are independent from each other. Supp-Tab. 2 (Supplementary 5) shows the Pearson correlation r between the parameters investigated in this study. Focus is on parameters with numerical units. Therefore, qualitative parameters such as the islands' material or observation of pumice were not considered in the correlation analysis.

The islands' area and the eruption duration show a significant positive correlation. This can be explained by the fact that long-lasting eruptions naturally produce a greater amount of material. There is a strong link between the eruption duration and the islands' area and volume, with the latter showing a positive, but not significant correlation with the eruption duration. Naturally, the parameters island area and volume are closely linked to each other as shown by the significant positive correlation ($r = 0.88$). As the percentage of daily erosion rate (in 2D and 3D) is calculated using the islands' area or volume (cf. Table 2), respectively, there exists a strong (negative) correlation between the parameters area and volume with the erosion parameters. As between area and volume, there is also a strong significant correlation between the percentage erosion rate measured in 2D and in 3D ($r = 1$).

Eruptions with a higher VEI seem to produce larger islands as shown by the significant positive correlation of $r = 0.61$ between VEI and area. The lower correlation between VEI and island volume could be explained by its smaller sample size.

The limited number of samples and the non-linear relationship between some of the parameters (e.g., island lifetime and area or volume), does not allow for a quantitative analysis such as multiple linear regression.

Conclusions

By investigating the evolution of 24 newly formed islands across 12 volcanic systems in the North Atlantic, the Western and Northern Pacific, and the Red Sea, this study analyzed the factors that influence the lifetime of a volcanic island.

Starting with the well-known Surtsey Island, formed south off the coast of Iceland in 1963, we combined multi-sensor satellite data time series (thermal, optical, and SAR data) with information from the scientific literature and databases such as the Global Volcanism Program to collect information on the islands' lifetime; eruption style, material, and duration (including thermal activity and the occurrence of floating pumice); island shape, area, and volume and their evolution over time; erosion rate; and the islands' climate and environment (wave height).

Based on this comprehensive dataset, we tested eight hypotheses about factors influencing the lifetime of a newly formed volcanic island. The "Discussion of hypotheses" section shows that the islands' lifetime is determined by a combination of different factors. Naturally, an island of a larger volume has a higher chance for a longer lifetime, assuming the same material. But we could show that the hypothesis "larger islands live longer" (hypothesis H1) is not always true. Small lava dome islands existed several years to decades—much longer than other islands of double and larger areas formed of unconsolidated tephra that were eroded within less than one year.

The material (unconsolidated pyroclastic tephra vs. hard lava) that the island is initially made of is important (hypothesis H5). However, independent of its material, to have a chance to withstand erosion in the initial post-eruption phase, an island also needs to exceed minimum area and volume thresholds (hypothesis H1). The exact thresholds for these parameters are also influenced by the material.

Our data further indicate that, while a longer eruption duration is not required to form a long-lasting island, longer eruption duration (hypothesis H3) correlates with a longer lifetime as it is typical for effusive eruptions to produce hard lava that is more resistant to ocean erosion. Moreover, growth of an island over several eruption episodes every few months or years generally supports a longer lifetime (hypothesis H4). However, this does not hold in cases where the renewed activity includes destructive explosive eruption. If an island was big enough after the initial eruption to live long enough for hydrothermal activity to alter unconsolidated pyroclastic tephra to palagonite tuff, it can become more resistant to wave erosion (hypothesis H6). This extends the lifetime of an island.

The influence that the island's shape has on its lifetime (hypothesis H2) cannot be determined due to the limited number of available samples. The hypothesis H7 about the potential protection by long-term stable beaches or older islands in the direct neighborhood cannot be confirmed. Further, an environment of calm wind and small waves (hypothesis H8) supports a long island lifetime.

We have generated an initial database to investigate the relationship between the lifetime of volcanic islands and 18 parameters for 24 islands reaching back to 1963. This database is available as Supp-Tab. 1. It will grow as more observations are made, allowing more opportunities for future analysis. Future work could extend this database by investigating further parameters such as the slope of the submarine edifice and the pre-eruption water depth at the summit.

The upcoming SAR mission Harmony will contribute to a more regular observation of topographic changes on volcanoes. In addition, prompt tasking of VHR optical stereo data is required for a detailed documentation of the fast and dynamic evolution of new volcanic islands. Regular and systematic 3D satellite data are the key for quantitative observations that allow us to better understand the processes of volcanic island formation and evolution.

Supplementary Information The online version contains supplementary material available at https://doi.org/10.1007/s00445-026-01987-5.

Acknowledgements TerraSAR-X data were provided by the German Aerospace Center (DLR). RapidEye and PlanetScope data were provided by Planet Labs. WorldView data were provided by European Space Imaging via European Space Agency (ESA) Third Party Mission Proposal ID 70735. Review comments by Christopher F. Waythomas (Alaska Volcano Observatory, USGS), by Alessandro Fornaciai (INGV) and by an anonymous reviewer are appreciated and helped to improve the clarity of the manuscript. Any use of trade, firm, or product names is for descriptive purposes only and does not imply endorsement by the U.S. Government.

Author contribution S.P. conceived this study, processed and analyzed the SAR, multispectral and thermal satellite data. N.G. processed and analyzed the Himawari data. S.P. wrote the first draft of the manuscript. R.G., H.R.D., U.K., F.J.M., H.T. and T.R.W. contributed to the writing. F.M., N.P., E.C., N.G., S.M. and T.U. supported the study. All authors discussed the results, commented on the manuscript, and gave final approval for publication.

Funding Open Access funding enabled and organized by Projekt DEAL.

Data availability Quantitative parameters following Table 2 are available as a database (see Supplementary Table 1). Original satellite data are available via DLR (TerraSAR-X: [https://sss.terrasar-x.dlr.de/]), NASA (MODIS & VIIRS: [https://firms.modaps.eosdis.nasa.gov/]), Landsat: [https://earthexplorer.usgs.gov/]), Planet Labs (PlanetScope & RapidEye: [https://www.planet.com/]), European Space Imaging (WorldView: [https://www.euspaceimaging.com/]), ESA (Sentinel-2:

[https://dataspace.copernicus.eu/]) and CEReS (Center for Environmental Remote Sensing) of Chiba University—Japan (Himawari 8/9 gridded data: [ftp://hmwr829gr.cr.chiba-u.ac.jp/gridded/FD/]). Climatological data used are available at [https://climatecharts.net/]). ERA5 wave data of the ECWMF ("mean wave direction" and "significant height of combined wind waves and swell") are available via the Copernicus Climate Data Store ([https://cds.climate.copernicus.eu/]). Wind data used are available via the Global Wind Atlas ([https://globalwindatlas.info]).

Declarations

Disclaimer Any use of trade, firm, or product names is for descriptive purposes only and does not imply endorsement by the U.S. Government.

Competing interests The authors declare no competing interests.

References

Angarita M, Grapenthin R, Plank S, Meyer FJ, Dietterich H (2022) Quantifying large-scale surface change using SAR amplitude images: crater morphology changes during the 2019–2020 Shishaldin Volcano eruption. J Geophys Res Solid Earth 127(8). https://doi.org/10.1029/2022JB024344

Begét J, Kienle J (1992) Cyclic formation of debris avalanches at Mount St Augustine volcano. Nature 356:701–704. https://doi.org/10.1038/356701a0

Bryan SE, Cook A, Evans JP, Colls PW, Wells MG, Lawrence MG, Jell JS, Greig A, Leslie R (2004) Pumice rafting and faunal dispersion during 2001–2002 in the Southwest Pacific: record of a dacitic submarine explosive eruption from Tonga. Earth Planet Sci Lett 227(1–2):135–154. https://doi.org/10.1016/j.epsl.2004.08.009

Cavallaro D, Coltelli M (2019) The Graham Volcanic Field offshore southwestern Sicily (Italy) revealed by high-resolution seafloor mapping and ROV images. Front Earth Sci 7:311. https://doi.org/10.3389/feart.2019.00311

Coombs M, Wallace K, Cameron C, Lyons J, Wech A, Angeli K, Cervelli P (2019) Overview, chronology, and impacts of the 2016–2017 eruption of Bogoslof volcano, Alaska. Bull Volcanol 81. https://doi.org/10.1007/s00445-019-1322-9

Copernicus Climate Data Store https://cds.climate.copernicus.eu/, https://codes.ecmwf.int/grib/param-db/140229. Accessed on August 4, 2025

Coppola D, Barsotti S, Cigolini C, Laiolo M, Pfeffer MA, Ripepe M (2019) Monitoring the time-averaged discharge rates, volumes and emplacement style of large lava flows by using MIROVA system: the case of the 2014–2015 eruption at Holuhraun (Iceland). INGV Ann Geophys 61:1–29. https://doi.org/10.4401/ag-7749

Decker R, Decker B (1981) Volcanoes, 1st edn.. W. H. Freeman, San Francisico

Fanti V, Ferreira Ó, Kümmerer V, Loureiro C (2023) Improved estimates of extreme wave conditions in coastal areas from calibrated global reanalyses. Commun Earth Environ 4(1). https://doi.org/10.1038/s43247-023-00819-0

Fauria KE, Jutzeler M, Mittal T, Gupta AK, Kelly LJ, Rausch J, Bennartz R, Delbridge B, Retailleau L (2023) Simultaneous creation of a large vapor plume and pumice raft by the 2021 Fukutoku-Oka-no-Ba shallow submarine eruption. Earth Planet Sci Lett 609. https://doi.org/10.1016/j.epsl.2023.118076

FIRMS. Fire-Information-for-Resource-Management-System (2025) https://firms.modaps.eosdis.nasa.gov. Accessed on April 4, 2025

Fridriksson S (1975) Surtsey: evolution of life on a volcanic island, 1st edn.. Butterworth & Co, London, 198

Gao G, Walter TR, Müller D, Marzban P, Plank S (2025) Applications and implications of monitoring surface hydrothermal deposits at Lastarria Volcano, Chile, using multispectral satellite data and cloud computing. Geothermics 127. https://doi.org/10.1016/j.geothermics.2025.103255

Garvin JB, Slayback DA, Ferrini V, Frawley J, Giguere C, Asrar GR, Andersenet K (2018) Monitoring and modeling the rapid evolution of Earth's newest volcanic island: Hunga Tonga Hunga Ha'apai (Tonga) using high spatial resolution satellite observations. Geophys Res Lett 45:3445–3452. https://doi.org/10.1002/2017GL076621

Genzano N, Marchese F, Plank S, Pergola N (2023) Monitoring the Mauna Loa (Hawaii) eruption of November–December 2022 from space: results from GOES-R, Sentinel-2 and Landsat-8/9 observations. Int J Appl Earth Obs Geoinf 122. https://doi.org/10.1016/j.jag.2023.103388

Geospatial Information Authority of Japan GSI (2023) https://www.gsi.go.jp/ENGLISH/. Accessed on August 13, 2025

Giglio L, Schroeder W, Justice CO (2016) The collection 6 MODIS active fire detection algorithm and fire products. Remote Sens Environ 178:31–41. https://doi.org/10.1016/j.rse.2016.02.054

Global Volcanism Program (2025a) [Database] Volcanoes of the World (v. 5.3.1; 6 Aug 2025). Distributed by Smithsonian Institution, compiled by Venzke, E. https://doi.org/10.5479/si.GVP.VOTW5-2025.5.3. Accessed on May 22, 2025

Global Volcanism Program (2025b) Zubair Group in Volcanoes of the World (v. 5.3.1; 6 Aug 2025). Distributed by Smithsonian Institution, compiled by Venzke, E. https://volcano.si.edu/volcano.cfm?vn=221020. Accessed on May 22, 2025

Global Volcanism Program (2025c) Home Reef in volcanoes of the world (v. 5.3.1; 6 Aug 2025). Distributed by Smithsonian Institution, compiled by Venzke, E. https://volcano.si.edu/volcano.cfm?vn=243080. Accessed on May 22, 2025

Global Volcanism Program (2025d) Late'iki in Volcanoes of the World (v. 5.3.1; 6 Aug 2025). Distributed by smithsonian institution, compiled by Venzke, E. https://volcano.si.edu/volcano.cfm?vn=243070. Accessed on May 22, 2025

Global Volcanism Program (2025f) Kuwae in Volcanoes of the World (v. 5.3.1; 6 Aug 2025). Distributed by Smithsonian Institution, compiled by Venzke, E. https://volcano.si.edu/volcano.cfm?vn=257070. Accessed on May 22, 2025

Global Volcanism Program (2025e) Hunga Tonga-Hunga Ha'apai in Volcanoes of the World (v. 5.3.1; 6 Aug 2025). Distributed by Smithsonian Institution, compiled by Venzke, E. https://volcano.si.edu/volcano.cfm?vn=243040 . Accessed on May 22, 2025

Global Volcanism Program (2025h) Fukutoku-Oka-no-Ba in Volcanoes of the World (v. 5.3.1; 6 Aug 2025). Distributed by Smithsonian Institution, compiled by Venzke, E. https://volcano.si.edu/volcano.cfm?vn=284130. Accessed on May 22, 2025

Global Volcanism Program (2025i) Iwo Jima / Ioto in Volcanoes of the World (v. 5.3.1; 6 Aug 2025). Distributed by Smithsonian

Institution, compiled by Venzke, E. https://volcano.si.edu/volcano.cfm?vn=284120. Accessed on May 22, 2025

Global Volcanism Program (2025g) Kavachi in Volcanoes of the World (v. 5.3.1; 6 Aug 2025). Distributed by Smithsonian Institution, compiled by Venzke, E. https://volcano.si.edu/volcano.cfm?vn=255060. Accessed on May 22, 2025

Global Volcanism Program (2025j) Nishinoshima in Volcanoes of the World (v. 5.3.1; 6 Aug 2025). Distributed by Smithsonian Institution, compiled by Venzke, E. https://volcano.si.edu/volcano.cfm?vn=284096. Accessed on May 22, 2025

Global Volcanism Program (2025k) Bogoslof in Volcanoes of the World (v. 5.3.1; 6 Aug 2025). Distributed by Smithsonian Institution, compiled by Venzke, E. https://volcano.si.edu/volcano.cfm?vn=311300. Accessed on May 22, 2025.

Global Wind Atlas https://globalwindatlas.info. Accessed on August 5, 2025

Heap MJ, Geyer A, Dibben J, Hickey J, Gisbert G, Vilanova-Pagès O, Ibañez-Insa J, Polo-Sánchez A, Giralt S, Moulin M, Álvarez-Valero AM (2025) Petrophysical properties of hydrothermally-altered pyroclastic deposits from Deception Island (Bransfield Strait, Antarctica). J Volcanol Geotherm Res 466. https://doi.org/10.1016/j.jvolgeores.2025.108399

Hersbach H, Bell B, Berrisford P, Hirahara S, Horányi A, Muñoz-Sabater J et al (2020) The ERA5 global reanalysis. Q J R Meteorol Soc 146(730):1999–2049. https://doi.org/10.1002/qj.3803

Holthuijsen LH (2007) Waves in oceanic and coastal waters. Cambridge University Press. https://doi.org/10.1017/CBO9780511618536

IFSAR DEM Intermap Technologies Inc (2018) http://www.intermap.com/. Accessed on May 23, 2025

Jackson MD, Heap MJ, Vola G, Ardit M, Rhodes JM, Peterson JG, Tamura N, Gudmundsson MT (2024) Material and mechanical properties of young basalt in drill cores from the oceanic island of Surtsey, Iceland. Geol Soc Am Bull 136(9–10):3527–3552. https://doi.org/10.1130/B37037.1

Jakobsson SP (1972) On the consolidation and palagonitization of the tephra of the Surtsey volcanic island, Iceland. Surtsey Res Prog Rep VI:121–129

Jakobsson SP (1978) Environmental factors controlling the palagonitization of the Surtsey tephra, Iceland. Bull Geol Soc Den 27:91–105

Jakobsson SP, Gudmundsson G, Moore JG (2000) Geological monitoring of Surtsey, Iceland. Surtsey Res 11:99–108

Kokelaar BP (1983) The mechanism of Surtseyan volcanism. J Geol Soc London 140:939–944. https://doi.org/10.1144/gsjgs.140.6.0939

Maeno F, Yasuda A, Hokanishi N et al (2021) Intermittent growth of a newly-born volcanic island and its feeding system revealed by geological and geochemical monitoring 2013–2020, Nishinoshima, Ogasawara, Japan. Front Earth Sci 9. https://doi.org/10.3389/feart.2021.773819

Maeno F, Kaneko T, Ichihara M, Suzuki YJ, Yasuda A, Nishida K, Ohminato T (2022) Seawater-magma interactions sustained the high column during the 2021 phreatomagmatic eruption of Fukutoku-Oka-no-Ba. Comm Earth & Environ 3:260. https://doi.org/10.1038/s43247-022-00594-4

Mantas VM, Pereira AJSC, Morais PV (2011) Plumes of discolored water of volcanic origin and possible implications for algal communities. The case of the Home Reef eruption of 2006 (Tonga, Southwest Pacific Ocean). Remote Sens Environ 115:1341–1352. https://doi.org/10.1016/j.rse.2011.01.014

Matoza RS, Fee D, Assink JD, Iezzi AM, Green DN, Kim K et al (2022) Atmospheric waves and global seismoacoustic observations of the January 2022 Hunga eruption, Tonga. Science 377(6601):95–100. https://doi.org/10.1126/science.abo7063

Melson WG, Jarosewich E, Lundquist CA (1970) Volcanic eruption at Metis Shoal, Tonga, 1967–1968. Description and petrology. Smithson Contrib Earth Sci 4:1–18. https://doi.org/10.5479/si.00810274.4.1

Nagai M, Miwa T, Nakada S, Ueda H, Sumino H, Yasuda A, Kozono T, Hirose T, Minami H, Kobayashi T (2025) Outline of the 2022–2024 eruption at Ioto Island (Iwo-jima), Ogasawara, Japan: small subaqueous eruption associated with shallow magma intrusion towards the caldera floor. Book of abstracts, IAVCEI Scientific Assembly, Geneva, June 29 - July 4, 2025, page 858.

Nunn PD (1994) Oceanic islands, 1st edn.. Blackwell, Oxford UK & Cambrige USA

Óskarsson BV, Jónasson K, Valsson G, Belart JMC (2020) Erosion and sedimentation in Surtsey Island quantified from new DEMs. Surtsey Res 14:63–77. https://doi.org/10.33112/surtsey.14.5

Pappas O, Biggs J, Prats-Iraola P, Pulella A, Stinton A, Achim A (2025) Measuring topographic change after volcanic eruptions using multistatic SAR satellites: simulations in preparation for ESA's Harmony mission. Remote Sens Environ 317. https://doi.org/10.1016/j.rse.2024.114528

Perron JT (2017) Climate and the pace of erosional landscape evolution. Annu Rev Earth Planet Sci 45(1):561–591. https://doi.org/10.1146/annurev-earth-060614-105405

PlanetLabs (2025) https://developers.planet.com/docs/data/planetscope/. Accessed on July 4, 2025

Plank S, Walter TR, Martinis S, Cesca S (2019) Growth and collapse of a littoral lava dome during the 2018/19 eruption of Kadovar Volcano, Papua New Guinea, analyzed by multi-sensor satellite imagery. J Volcanol Geotherm Res 388. https://doi.org/10.1016/j.jvolgeores.2019.106704

Plank S, Marchese F, Genzano N, Nolde M, Martinis S (2020) The short life of the volcanic island New Late'iki (Tonga) analyzed by multi-sensor remote sensing data. Sci Rep 10(1):1–15. https://doi.org/10.1038/s41598-020-79261-7

Plank S, Shevchenko AV, d'Angelo P, Gstaiger V, González PJ, Cesca S, Martinis S, Walter TR (2023) Combining thermal, tri–stereo optical and bi–static InSAR satellite imagery for lava volume estimates: the 2021 Cumbre Vieja eruption, La Palma. Sci Rep 13. https://doi.org/10.1038/s41598-023-29061-6

Plank S, Ciancia E, Genzano N, Falconieri A, Martinis S, Taubenböck H, Pergola N, Marchese F (2025) The evolution of the 2022–2024 eruption at Home Reef, Tonga, analyzed from space shows vent migration due to erosion. Sci Rep 15. https://doi.org/10.1038/s41598-025-95197-2

Poland MP (2014) Time-averaged discharge rate of subaerial lava at Kīlauea Volcano, Hawai'i, measured from TanDEM-X interferometry: implications for magma supply and storage during 2011–2013. J Geophys Res Solid Earth 119:5464–5481. https://doi.org/10.1002/2014JB011132

Poland MP, Lopez T, Wright R, Pavolonis MJ (2020) Forecasting, detecting, and tracking volcanic eruptions from space. Remote Sens Earth Syst Sci 3. https://doi.org/10.1007/s41976-020-00034-x

Prause S, Weisenberger TB, Kleine BI, Monien P, Rispoli C, Stefánsson A (2022) Alteration of basaltic glass within the Surtsey hydrothermal system, Iceland – implication to oceanic crust seawater interaction. J Volcanol Geotherm Res 429. https://doi.org/10.1016/j.jvolgeores.2022.107581

Ramalho RS, Quartau R, Trenhaile AS, Mitchell NC, Woodroffe CD, Ávila SP (2013) Coastal evolution on volcanic oceanic islands: a complex interplay between volcanism, erosion, sedimentation, sea-level change and biogenic production. Earth-Sci Rev 127:140–170. https://doi.org/10.1016/j.earscirev.2013.10.007

Romagnoli C, Jakobsson SP (2015) Post-eruptive morphological evolution of island volcanoes: Surtsey as a modern case study.

Geomorphology 250:384–396. https://doi.org/10.1016/j.geomorph.2015.09.016
Schmidt R, Schmincke H-U (2000) Seamounts and island building. In: Sigurdsson H (ed) Encyclopedia of volcanoes. Academic Press, San Diego, pp 383–402
Schmidt R, Schmincke H-U (2002) From seamount to oceanic island, Porto Santo, central East-Atlantic. Int J Earth Sci (Geol Rundsch) 91:594–614. https://doi.org/10.1007/s00531-001-0243-x
Schroeder W, Oliva P, Giglio L, Csiszar IA (2014) The new VIIRS 375m active fire detection data product: algorithm description and initial assessment. Remote Sens Environ 143:85–96. https://doi.org/10.1016/j.rse.2013.12.008
Thorarinsson S (1964) Surtsey: the new island in the North Atlantic. Almenna Bókafélagid, Reykjavik
Vaughan RG, Webley PW (2010) Satellite observations of a Surtseyan eruption: Hunga Ha'apai, Tonga. J Volcanol Geotherm Res 198:177–186. https://doi.org/10.1016/j.jvolgeores.2010.08.017
Walker GPL (1973) Explosive volcanic eruptions a new classification scheme. Geol Rundsch 62:431–446
Walter TR (2023) Radar sensing of Merapi Volcano. In: Gertisser R, Troll VR, Walter TR, Nandaka IGMA, Ratdomopurbo A (eds) Merapi Volcano. Active Volcanoes of the World. Springer, Cham. https://doi.org/10.1007/978-3-031-15040-1_14
Walter TR, Haghshenas Haghighi M, Schneider FM et al (2019) Complex hazard cascade culminating in the Anak Krakatau sector collapse. Nat Commun 10. https://doi.org/10.1038/s41467-019-12284-5
Wang J, Wang Y (2021) Evaluation of the ERA5 significant wave height against NDBC buoy data from 1979 to 2019. Mar Geod 45(2):151–165. https://doi.org/10.1080/01490419.2021.2011502
Waythomas CF, Scott WE, Nye CJ (2010) The geomorphology of an Aleutian volcano following a major eruption: the 7–8 August 2008 eruption of Kasatochi Volcano, Alaska, and its aftermath. Arct Antarct Alp Res 42(3):260–275. https://doi.org/10.1657/1938-4246-42.3.260
Waythomas CF, Angeli K, Wessels RL (2020) Evolution of the submarine–subaerial edifice of Bogoslof volcano, Alaska, during its 2016–2017 eruption based on analysis of satellite imagery. Bull Volcanol 82. https://doi.org/10.1007/s00445-020-1363-0
Waythomas CF, Loewen M, Wallace KL et al (2020) Geology and eruptive history of Bogoslof volcano. Bull Volcanol 82. https://doi.org/10.1007/s00445-019-1352-3
Wright R (2016) MODVOLC: 14 years of autonomous observations of effusive volcanism from space. In: Harris AJL (ed) Detecting, modelling and responding to effusive eruptions. Geological Society, London, pp 23–53
Xu W, Ruch J, Jónsson S (2015) Birth of two volcanic islands in the southern Red Sea. Nat Commun 6. https://doi.org/10.1038/ncomms8104
Yeo IA, McIntosh IM, Bryan SE, Tani K, Dunbabin M, Metz D, Collins PC, Stone K, Manu MS (2022) The 2019–2020 volcanic eruption of Late'iki (Metis Shoal), Tonga. Sci Rep 12. https://doi.org/10.1038/s41598-022-11133-8
Zepner L, Karrasch P, Wiemann F, Bernard L (2020) ClimateCharts.net – an interactive climate analysis web platform. Int J Digit Earth 14(3):338–356. https://doi.org/10.1080/17538947.2020.1829112
Zimanowski B, Büttner R, Dellino P, White JDL, Wohletz KH (2015) Chapter 26 - magma–water interaction and phreatomagmatic fragmentation. In: Sigurdsson H (ed) The Encyclopedia of Volcanoes, 2nd edn. Academic Press, pp 473–484